Maria Elias Lopes Pereira

Bachelor in Micro and Nanotechnologies Engineering

Characterization of direct X-ray Detectors based on Organic Semiconductor thin films

Dissertation submitted in partial fulfillment
of the requirements for the degree of

Master of Science in
Micro and Nanotechnologies Engineering

Adviser: Dr. Pedro Barquinha, Associate Professor,
Faculty of Sciences and Technology, NOVA University of Lisbon,

Co-adviser: Dr. Beatrice Fraboni, Associate Professor,
Department of Physics, Alma Mater Studiorum, University of Bologna

Examination committee:

Committe chair: Prof. Dr. Rodrigo Martins

Examiner: Prof. Dr. Joana Sarmento

FACULDADE DE CIÊNCIAS E TECNOLOGIA
UNIVERSIDADE NOVA DE LISBOA

September, 2018

Characterization of direct X-ray Detectors based on Organic Semiconductor thin films

Pedra sobre pedra, sobre o sal
do corpo. Colunas, muros
castelos. Testemunhos
marcas de água.

"Marcas de Água" de Vasco Pontes

Acknowledgements

In this first part I would like to acknowledge everybody that in some way were important not only to the conclusion of this project, but also throughout the entire path that lead me here.

Firstly, I would like to thank Professor Rodrigo Martins and Professor Elvira Fortunato for the creation of the Micro and Nanotechnology course! It is, in fact, "o curso do futuro", composed by Senhores, Sonhadores e Doutores. Thank you for giving us students the chance to learn with some of the best researchers in this field. Thank you for allowing us to be in contact with some of the most high-tech machines and equipment, in such a way that we don't even realize how extraordinary they are until we visit other labs. Thank you for making Portugal noticed abroad for the excellence of CENIMATs work.

I obviously have to thank my adviser Professor Pedro Barquinha for all of his advices and help specially in the conclusion of this project. Mostly I have to thank his availability throughout this last year. I have to say, even though I was in a different country I never felt I was alone or unsupported.

Another important big appreciation goes to the University of Bologna and specially to Professor Beatrice Fraboni. Thank you so much for everything, receiving me so well, teaching me so much and guiding me with such patience. Thank you for allowing me to have this amazing experience abroad. I would like to also thank Professor Andrea Ciavatti for all the suggestions and help.

A special thanks to Ilaria Fratelli. You taught me how to work! You taught me how to be professional and perform. You taught me to deliver. You were my team in Bologna and the fact that we worked so well together is the reason I stayed motivated throughout the entire time I was there.

Tenho, pois claro, que agradecer à minha maravilhosa família! Ao meu pai, principalmente por toda a ajuda académica que sempre me deu e por ter lido a minha tese e mandado uns "bitaites" como se percebesse muito do assunto. À minha mãe, por sonhar por mim e para mim. A ambos, por serem os melhores do mundo. Acho que não era preciso mencionar, mas não teria alcançado nada se não fossem vocês. Agradeço ao meu irmão por acreditar em mim e me obrigar a ser melhor para merecer essa confiança. Agradeço aos meus avós por todo o apoio incondicional que nunca, nunca me faltou.

Por fim, tenho que agradecer a alguns amigos que me ajudaram e muito ao longo deste longo caminho que me trouxe até aqui. À Cláudia Bento, um grandessíssimo obrigada por tudo, sei que foste a pessoa que mais teve que aturar o meu mau humor e as minhas reclamações ao longo do curso. Foste sem dúvida o meu ombro amigo e a minha maior companhia em quase todas (mentira) as longas noites de estudo. Queria agradecer também ao meu grande amigo Miguel Ramos. Apesar de termos feito apenas a licenciatura juntos, és o meu amigo do curso e da vida na verdade! Obrigada por todas as vezes

que me acordaste para ir às aulas, por todas a vezes que me ajudaste a estudar e por toda a preocupação que sempre tiveste comigo. Ao Ricardo Correia e ao André Sá, porque quase todos os trabalhos de grupo ao longo destes 5 anos foram com vocês, e apesar de todo o stress envolvido sempre foi divertido. And finally, to the best roommate I could have asked for in Bologna, Massimiliano Bartoloni. You know it wasn't always easy to be away from home, but I hope you know that you were my family when I really needed. Thank you for treating me so well and teaching me so much.

Um último agradecimento a todas as pessoas que não pude enumerar, mas que de certa forma também contribuíram para a conclusão deste projeto e deste grande curso que é o meu.

Abstract

The detection of ionizing radiation such as X-rays is a constantly growing area of research thanks to its numerous application fields, which span from astrophysics, to industrial and civil security or even medical imaging and diagnostics. In this project, conducted at the University of Bologna (UNIBO), department of physics, one of the most active groups of research in this area, four different molecules (TIPS, TIPGe, diF TES ADT and diF TEG ADT) were studied as the organic semiconductor thin film in a photoconductor. The devices were realized by drop-casting a solution processed of the molecules onto three different substrates (PET, PEN and glass), for a direct approach on the detection of this radiation. Different parameters such as resistivity, percentage of active area covered by the molecule, quantity and thickness of the crystals, were investigated for their influence on the performance of the X-Ray detector.

It was found that in the PET substrate there is a process of discharge that seems to be important to the performance of the detector and that seems to induce a decrease in the current of the diF TES ADT and diF TEG ADT based devices, making them unsuitable for any kind of application.

With the PEN substrate it is possible to achieve reliable and reproducible devices with high signal to noise ratios and acceptable sensitivities.

The glass substrate with the TIPGe would be the best one because it combines a high sensitivity with a reliable and reproducible device. Nevertheless, glass is not a flexible substrate and therefore is not suitable for many of the applications of interest, for example wearable health diagnostic applications like a personal dosimeter.

Finally, it was proved that the molecules with the germanium element show, as it was expected due to the higher atomic number of Ge compared to Si, the highest sensitivities. It was also discovered that this is also due to the high quality crystals achieved with these molecules.

Given the results obtained, this line of research seems to be fruitful, with very interesting practical applications expected.

Keywords: X-Ray detection, organic semiconductor thin films, photoconductors, drop-casting

Resumo

A deteção de radiação ionizante, como os raios-X, é uma área de pesquisa em constante crescimento, graças aos seus vastos campos de aplicação, que abrangem desde a astrofísica, centrais nucleares, segurança industrial e civil, até ao diagnóstico médico. Neste projeto, realizado na Universidade de Bolonha, no departamento de física, um dos grupos de investigação mais ativos nesta área, quatro moléculas diferentes (TIPS, TIPGe, diF TES ADT e diF TEG ADT) foram estudadas na forma de filme fino orgânico semicondutor num fotocondutor. Os dispositivos foram preparados através da deposição por *drop-casting* de uma solução destas moléculas em três substratos (PET, PEN e vidro), para uma abordagem direta na deteção desta radiação. A influência de diferentes parâmetros, como a resistividade, percentagem de área ativa coberta pela molécula, quantidade e espessura dos cristais, foi investigada quanto ao desempenho dos detetores de raios-X.

Descobriu-se que, no substrato PET, há um processo de descarga que parece ser importante para o desempenho do detetor e que aparentemente induz uma diminuição na corrente dos dispositivos baseados em diF TES ADT e diF TEG ADT, tornando-os inadequados para qualquer tipo de aplicação.

Com o substrato PEN, é possível obter dispositivos fiáveis e reprodutíveis com baixo ruído e sensibilidades aceitáveis.

O substrato de vidro com o TIPGe daria o melhor dispositivo porque combina uma alta sensibilidade com um dispositivo fiável e reprodutível. No entanto, não é um substrato flexível e, portanto, não é adequado para muitas das aplicações de interesse, como por exemplo, aplicações de diagnóstico de saúde, como a dosimetria pessoal.

Finalmente, ficou provado que as moléculas com o elemento germânio apresentam, como esperado pelo seu número atómico mais elevado que o do silício, as mais altas sensibilidades. Descobriu-se, ainda, que isso também se deve aos cristais de alta qualidade obtidos nessas moléculas.

Em função dos resultados obtidos, a linha de investigação parece profícua, esperando-se aplicações práticas muito interessantes.

Palavras-chave: Deteção de Raios-X, filmes finos semiconductores orgânicos, fotocondutores, *drop-casting*

Contents

List of Figures

List of Tables

Acronyms

AFM	Atomic Force Microscope
CB	Chlorobenzene
diF TEG ADT	2,8-Difluoro-5,11-bis(triethylgermylethynyl)anthradithiophene
diF TES ADT	2,8-Difluoro-5,11-bis(triethylsilylethynyl)anthradithiophene
PLA	Planar geometry
SAC	Solvent assisted crystallization
PEN	Polyethylene naphthalate
PET	Polyethylene terephthalate
TIPGe	6,13-Bis(triisopropylgermylethynyl)pentacene
TIPS	6,13-Bis(triisopropylsilylethynyl)pentacene

Motivation and Objectives

Organic electronics is an emerging technology with promising applications where very high-performance semiconductor devices are not necessary but characteristics such as flexibility, biocompatibility, low fabrication costs and disposability are required. These applications could include disposable electronics, smart cards, light-emitting diodes, signage, wearable electronics and sensors. One of the appealing features of organic materials is the easy deposition over large areas by means of solution-coating, low-cost techniques, such as drop casting [1], inkjet printing [2][3], solution shearing [4], potentially onto flexible substrates [1][5]. Furthermore, to compete with flexible forms of inorganic semiconductors, such as ultra-thin single crystal silicon, these organic devices should also exhibit a very good electro-mechanical stability which means a mechanical flexibility without degradation of the electrical performance. Therefore organic electronics might allow the emergence of new applications in different fields, exploiting the unique properties of carbon-based materials which also makes them very promising for the successful integration of electronics in biological systems for medical and bioengineering applications [6] [7] .

Moreover, organic materials were first suggested for radiation detection in the early 1980s [8], and it has been proven that they are viable and promising candidates for the detection of higher energy photons (X- and gamma-rays). The detection of ionizing radiation such as X-rays is a continuously growing area of research due to its numerous application fields, which span from astrophysics, to industrial and civil security or even medical imaging and diagnostics. Consequently, the radiation detectors market is large, diverse and global. In fact, its value has been increasing in the last years and it is expected to continue to grow (Figure 0.1) [9]. At the moment, it stands at about $30 billion USD (United States Dollar). The market is divided into medical radiation detectors (66% market share), safety and monitoring detectors (14%) and specialty and custom detectors (20%).

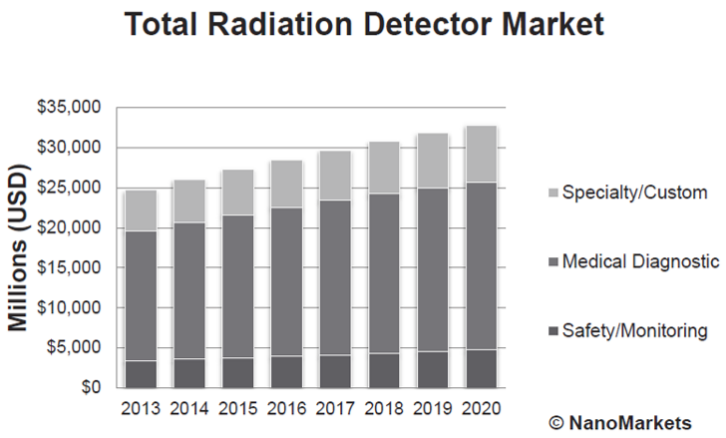

Figure 0.1: Radiation detectors total market. [9]

In this project, four different organic molecules (TIPS, TIPGe, diF TES ADT and diF TEG ADT) were studied as the organic semiconductor thin film in a photoconductor. The devices were realized by drop-casting a solution processed of the molecules onto three different substrates (PET, PEN and glass), for a direct approach on X-Rays detection. The main objectives were to find the best molecule/substrate combination in terms of performance as an X-ray detector, as well as a deeper understanding of the physical processes that occur in these organic materials when exposed to X radiation. The experimental work was conducted at the University of Bologna (UNIBO), department of physics, one of the most active groups of research in this area.

1 Introduction

In this first chapter, the main theoretical principles relevant to this work will be introduced. Since, in this project, several organic molecules were investigated for the detection of X-Rays, it is possible to find in subsection 1.1 a brief resume of the fundamental properties of organic materials and its use in electronics. In subsection 1.2, the general requirements of a radiation detector are explained and in subsection 1.3 an overview on organic semiconductor detectors based on thin films is presented.

1.1 Organic electronics

1.1.1 Organic materials

The key element in organic compounds is the Carbon atom, generally bonded to other atoms such as Hydrogen, Nitrogen, Oxygen, etc. The carbon atom is characterized by 6 electrons distributed as $1s^2\,2s^2\,2p^2$. It is very common that one of the two $2s^2$ electrons jump into the free $2p_z$ orbital, thus leading to four valence electrons, $2s\ 2p_x\ 2p_y\ 2p_z$[10]. Hybridization, introduced by Linus Pauling in 1931 [8], is a "mix" of these atomic orbitals which results in the formation of new, isoenergetic orbitals more suitable for the description of a specific molecule structure [11].

When a carbon atom has four single bonds, the 2s-orbital and the three 2p-orbitals hybridize and form four equivalent sp3-orbitals, equally shaped. All bonds between s-orbitals or hybrids of s-orbitals and p-orbitals are called σ-bonds. When one 2s-orbital combines with two of the three 2p-orbitals, three hybrid sp2-orbitals will be formed. As a result, there will be three sp2-orbitals lying on the same plane and one unhybridized (2pz), that is standing perpendicular. When two sp2 hybridized carbon atoms bond to each other, the sp2-orbitals will overlap forming the so called σ-bond. At the same time, the unhybridized pz-orbitals will start interacting too, forming a different kind of bond, called π-bond. These two types of covalent bonds (σ-bonds and π-bonds) are illustrated in Figure 1.1.

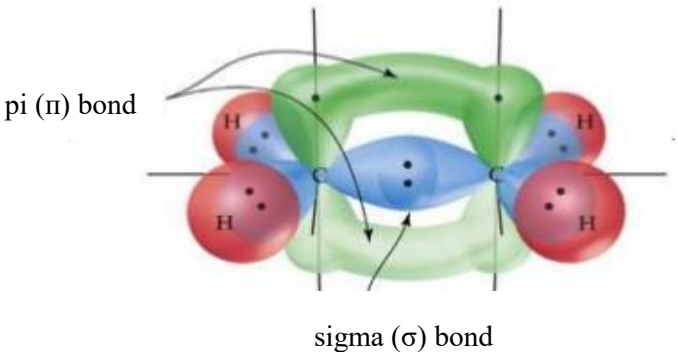

Figure 1.1: Two carbon atoms approach each other and form one pi bond and sigma bonds. [12]

In Figure 1.1. it is clear that σ electrons are strictly confined into the small volume between the two carbon atoms nuclei while π electrons are able to move into a larger volume and therefore its interaction with the nuclei is relatively weak[11][13]. This means that in σ-bonds the electrons involved are too localized to be free to move and therefore are not involved in charge transport mechanism. On the contrary, π-bonds are very weak and the electrons involved are much delocalized so that they can freely move across the molecule, in particular when an electric field is applied [10].

It is possible to separate the molecular energy levels into two categories: π and π×, bonding and anti-bonding respectively, forming a band-like structure (Figure 1.2). The occupied π-levels are the equivalent of the valence band in inorganic semiconductors.

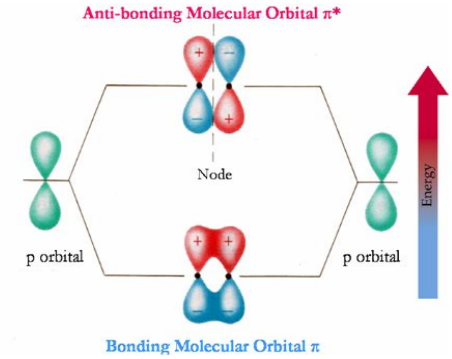

Figure 1.2: Bonding and anti-bonding π molecular orbitals [10].

The electrically active level is the highest one and it is called Highest Occupied Molecular Orbital (HOMO). The unoccupied π×-levels are equivalent to the conduction band. In this case, the electrically active level is the lowest one, called Lowest Unoccupied Molecular Orbital (LUMO). The resulting band gap is given by the difference of the energy between HOMO and LUMO.

1.1.2 Charge carrier transport in organic semiconductors

Organic semiconductors can be broadly classified into two categories: small molecules or oligomers (usually processed in vacuum) and polymers (usually processed by wet chemical techniques), varying from almost perfect crystals to amorphous solids. As a consequence, charge carrier transport in such solids varies in a range delimited by two extreme cases: band transport and hopping [11] [14].

Band transport is normally observed only in pure, single organic crystals, while for highly disordered polymeric solids the transport usually proceeds via hopping and is thermally activated. In amorphous solids, charge flow takes place when electrons start moving (hopping) from lower energy levels to higher energy levels. This flow is due to an increment in electrons energy which may be caused both by temperature or the application of an external electric field. [11]

The case of semicrystalline polymeric solids is perhaps the most complicated, from an analytical point of view. These solids usually assume a polycrystalline structure, in other words they may be thought of as many crystalline grains immersed into an amorphous matrix. While within the grains charges move thanks to band transport, the problem arises in correspondence with the grain boundaries. Here, mobile charges are temporarily immobilized (trapping) thus creating a potential barrier which electrostatically repels same sign charges; as a consequence, charge mobility is greatly decreased. [11]

In all instances, the performance of organic materials critically depends on the efficiency with which charge carriers (electrons and/or holes) move within the π -conjugated materials [14]. For charge transport in organic solids to occur, there must be a charge on the molecular unit. This may either be an additional electron that is accommodated in an antibonding orbital, or one that is removed from a bonding orbital. The molecule is then no longer in the ground state but rather in a charged excited state. The addition or removal of an electron from the molecule may be obtained in several ways. The most common is through injection or extraction of an electron at the interface between a metal electrode and the molecule[15].

1.1.3 Charge carrier injection into organic semiconductors

In electronic devices based on organic semiconductors, metal/organic semiconductor interfaces are very important and can strongly influence both the type and the amount of charge carrier injected into the channel. Charge injection strongly depends on the energy level matching between the Fermi level of the metal electrodes and organic semiconductors energy levels, namely, LUMO and HOMO, as described by the Mott-Schottky model. When a neutral metal and a neutral semiconductor are brought in contact, the Mott-Schottky model predicts that their bulk Fermi levels will align, causing band bending in the semiconductor (Figure 1.3) [10] [14].

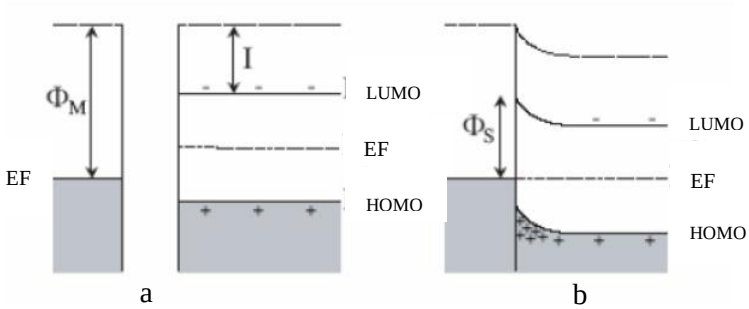

Figure 1.3: a) Metal (left) and Intrinsic semiconductor (right) that are not in contact; b) Metal/semiconductor contact, with band bending region in the semiconductor. EF indicates the position of the Fermi level. [10]

There are several aspects that can modify the Mott-Schottky-type of band bending. One of these is the formation of surface dipoles at the interface between the metal and the organic semiconductor. Another aspect that can have a strong influence in charge injection is the presence of traps at the metal/organic interface that are mostly produced during contact fabrication [10].

1.2 Radiation detection

X-rays are a form of electromagnetic radiation with a wavelength ranging from 0.01 to 10 nanometers, corresponding to frequencies in the range 30 petahertz to 30 exahertz (3×10^{16} Hz to 3×10^{19} Hz) and energies in the range 100 eV to 100 keV. They were first described by Wilhelm Röntgen in 1895, who discovered that X-rays could help visualize bones, and shortly after that they were being used in a medical setting. [16]

The detection of ionizing radiation such as X-rays is a constantly growing area of research thanks to its vast and numerous application fields, which span from astrophysics to nuclear power plants, to

industrial and civil security and to medical imaging and diagnostics. High energy photons (X- and gamma-rays) can be detected with two different categories of functional materials: scintillators and semiconductors. The first group of materials are used in the indirect conversion approach because they first convert ionizing radiation into visible photons that escape the scintillator and are collected by a coupled photo-multiplier tube (PMT) or a photodiode to, only then, obtain an electrical signal. The direct conversion of ionizing radiation into an electrical signal within the same device, achieved with semiconductors materials, is a more effective process than the indirect one, since it improves the signal-to-noise ratio and it reduces the device response time. Both processes are illustrated in Figure 1.4.

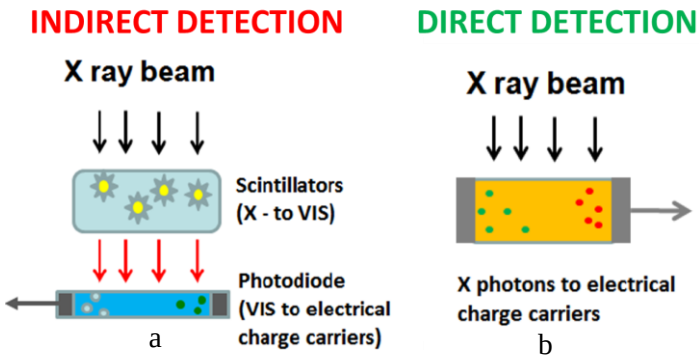

Figure 1.4: a) indirect process and b) direct process of X-Ray conversion into an electrical signal. [17]

In both cases, the interaction with a high energy photon first induces primary excitations and ionization processes (ions and electrons) which, at a second stage, interact within the volume of the detection material and produce a majority of secondary excitations (electron–hole pairs), within a picosecond timeframe. [18]

Given the fact that X-Rays are uncharged radiation, in order to detect it and possibly measure its quantity, this radiation must first undergo an interaction that radically alters the properties of the incident radiation in a single encounter. In all cases of practical interest, the interaction results in the full or partial transfer of energy of the incident radiation to electrons or nuclei of the constituent atoms, or to charged particle products of nuclear reactions. [19]

Although a large number of possible interaction mechanism are known for X-rays in matter, only two major types, called Photoelectric absorption and Compton scattering, play an important role in radiation measurements and both of them lead to the partial or complete transfer of the ray photon energy to electron energy. [19]

The photoelectric process is the predominant mode of interaction for X-rays. In this process, a photon undergoes an interaction with an absorber atom in which the photon completely disappears. In its place, an energetic photoelectron is ejected by the atom from one of its bound shells. [20]

In the Compton scattering interaction, the incoming ray photon is deflected through an angle with respect to its original direction. The photon transfers a portion of its energy to the electron (assumed to be initially at rest), which is then known as a recoil electron. [19]

Assuming that the incident radiation goes through one of these processes, it is now necessary a good detector. The main requirements for a good solid state semiconductor detector are briefly detailed below:

- High sensitivity, which is defined as the ionization charge collected per unit absorbed dose (usually in units of nC/Gy). Gray is the unit that quantifies the absorbed dose. One Gray is equivalent to one Joule per Kilogram. The sensitivity depends on temperature, dose rate and energy [21] [22];
- High resistivity ($>10^9$ Ω cm) and low leakage current are critical for low noise operation;
- Small enough band gap so that the electron–hole ionization energy is small (< 5 eV). This ensures that the number of electron–hole pairs created is reasonably large and results in a higher signal to noise ratio;
- High atomic number (Z) and/or a large interaction volume for efficient radiation–atomic interactions. For high-sensitivity and efficiency, large detector volumes are required to ensure that as many incident photons as possible have the opportunity to interact in the detector volume;
- High intrinsic μτ product. The carrier drift length is given by μτE, where μ is the carrier mobility, τ is the carrier lifetime and E is the applied electric field. Charge collection is determined by which fraction of photo-generated electrons and holes effectively traverses the detector and reaches the electrodes;
- High-purity, homogeneous, defect-free materials, to ensure good charge transport properties, low leakage currents, and no conductive short circuits between the detector contacts;

It is obvious that not all of the above requirements can be easily met by a single material, but the dramatic advancements in the organic semiconductor research field have recently stimulated studies on the potential application of organic semiconductors as solid-state detectors [18]. Moreover, the similarity of the typical density of organic molecules to that of human tissue makes them very interesting for medical X-ray direct dosimetry. [23]

1.3 X-Ray Detectors based on Organic Materials

As detectors of ionizing radiation, organic semiconductors have so far been mainly proposed in the indirect conversion approach, for example, as scintillators [24] [25], or as photodiodes [26] [27]. However, as stated before, the direct conversion of ionizing radiation into an electrical signal within the same device is a more effective process because it improves the signal to noise ratio and it reduces the device response time. [28]

In the last years, a few studies reported the proof-of-principle for direct X-ray detection based either on organic semiconducting single crystals [29] or on polymer thin-films blended either with p-conjugated small molecules [30], inorganic high-Z nanocomponents [31] or carbon nanotubes [32] to enhance the sensitivity to X-rays improving the charge carriers mobility and the stopping power of the material.

However, it has been difficult to achieve a system that combines the use of an organic semiconductor in a direct approach of X-Rays detection and that it is both flexible and works with ultra-low voltage bias. In 2016, it was discovered that this could all be possible using the 6,13-bis-(triisopropylsilylethynyl)pentacene (TIPS-pentacene) molecule (a standard material for the fabrication of organic devices onto flexible plastic substrates) deposited by drop casting onto flexible poly(ethyleneterephthalate) (PET) substrates. These devices revealed an unexpected high X-ray sensitivity. [1]

In this project, the starting point was this last finding and the main goal was to investigate the influence of different parameters in the sensitivity and, therefore, in the performance of the X-Ray detector. There is a similar molecule to TIPS which is called 6,13-bis(triisopropylgermylethynyl)pentacene (TIPGe-pentacene) and it only differs in one atom, which in TIPS is silicon and in TIPGe is germanium (Figure 1.5). Given that the germanium has a higher Z number, it is expected that this second molecule delivers better results than the TIPS as a detector for its higher absorption rate.

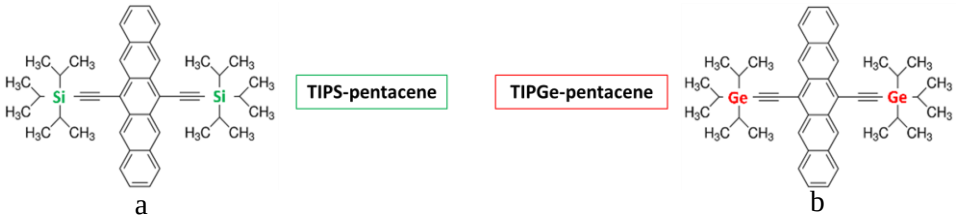

Figure 1.5: a) TIPS molecular structure and b) TIPGe molecular structure.

Another two similar molecules, with the same difference on the silicon becoming germanium, were tested to compare with the TIPS and TIPGe results. The chosen ones were the 2,8-Difluoro-5,11-bis(triethylsilylethynyl)anthradithiophene (diF TES ADT), because it has been proven to be a promising soluble semiconductor that has demonstrated a remarkable electronic performance as a thin film deposited by the drop casting method [33], and the 2,8-Difluoro-5,11-bis(triethylgermylethynyl)anthradithiophene (diF TEG ADT), being the germanium version of the diF TES ADT molecule (Figure 1.6).

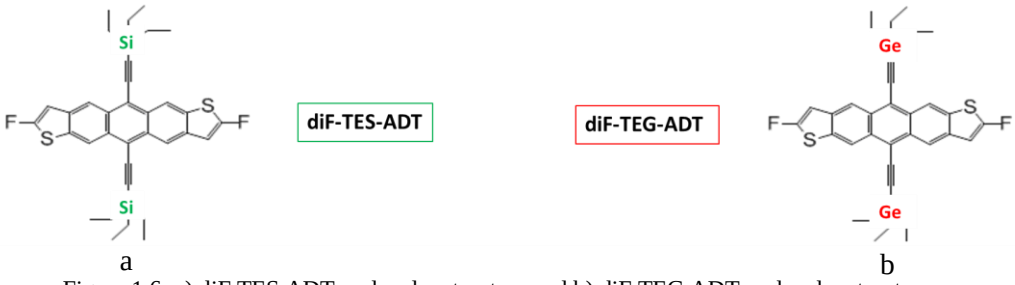

Figure 1.6: a) diF TES ADT molecular structure and b) diF TEG ADT molecular structure.

As all these four molecules are polymers, they have better mechanical flexibility and solution processability, when compared with small molecules, due to their long polymer chain (high molecular weight) and are consequently more compatible with plastic substrates [34]. For this reason, they were tested in three different substrates: PET, polyethylene naphthalate substrate (PEN) and glass for comparison. Given that PEN has a superior strength, a better heat stability and better barrier properties [35] it is expected to provide a better adhesion to the organic molecules and therefore the devices with this substrate should show better results. Also, it is known that carrier mobilities of 1.2 $cm^2/(Vs)$ were achieved in films fabricated by drop-casting TIPS-pentacene from toluene solution (the exact method used in this project) while mobilities of 0.1 $cm^2/(Vs)$ were obtained in diF TES ADT films [36]. This means that TIPS molecule has a better electrical performance, and therefore the carriers move more easily which should translate into a better X-Ray response than the diF TES ADT molecule. Similarly, the TIPGe molecule should give better results than the diF TEG ADT.

2 Methodology

In this chapter the general procedure adopted throughout the experimental work will be described. The samples preparation method, including description of materials and tools employed, will be treated in subsection 2.1. Subsequently, in subsection 2.2, the measurement setup will be described.

2.1 Sample preparation

In this work it was investigated the direct X-ray photoconversion process in organic thin film photoconductors (planar structure with two terminals).

In order to study and compare the effect of the substrate in the adhesion of the organic molecules, some of the samples were prepared in flexible polymeric substrates such as Polyethylene terephthalate (PET) or Polyethylene naphthalate (PEN) and others in a rigid substrate which was glass. The interdigitated gold electrodes were deposited and patterned over the substrate, before depositing the organic molecules. The Au interdigitated geometry on the PET substrate was W/L=50000µm/30µm. For the PEN and glass substrate, because it was fabricated in a different facility, the W/L was 205500µm/30µm. These electrodes were fabricated at Cagliari university and CENIMAT, respectively.

The deposition method used for the organic materials was the drop casting technique at room temperature in all the devices. The semiconductor solution (organic molecule) was prepared with a 0.5% of concentration in a chlorobenzene (CB) solvent in the case of diF TES ADT and diF TEG ADT, and 0.5% of concentration in a Toluene solvent for the TIPS and TIPGe molecules. The optimized volume deposited was 3µl of the organic solution, drop casted over the substrate. In Figure 2.1a, it is possible to find a scheme of the device structure and in Figure 2.1b/c the overall aspect of the various samples is illustrated.

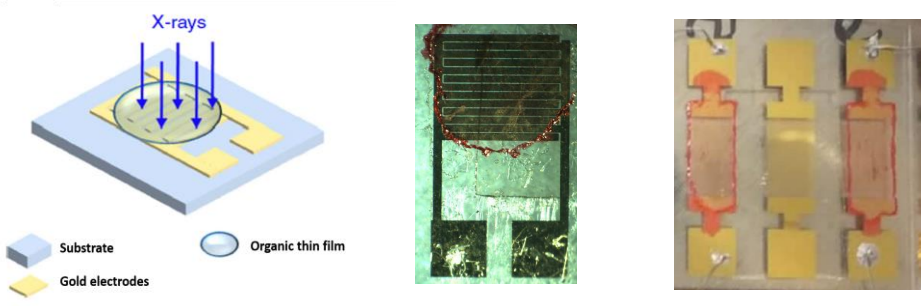

Figure 2.1: a) Schematic of the device structure. b) Photograph of one PET substrate c) Photograph of three substrates of PEN in which two of them were used for the deposition of the semiconductor.

After the deposition of the semiconductor, the samples were submitted to the SAC (Solvent Assisted Crystallization) method. This method consists in covering the samples for 1 hour next to 200 µl of CB or toluene (according to the molecule) at room temperature, immediately after the deposition. This creates a saturated environment which slows the crystallization of the semiconductor, resulting in bigger crystals. After one hour resting in the saturated environment, the samples were annealed at 90ºC for 1 hour in order to evaporate to whole solvent which allows for a better electrical performance (Figure 2.2.). Before the measurements of the devices, the samples stayed at rest protected from the light.

a b

Figure 2.2: a) SAC method b) Annealing.

2.2 X-Ray detection: Measurement setups and procedures

After the deposition process, all the samples were electrically characterized in a Probestation that was connected to a Keithley 2614B source measure unit. The current-voltage (I-V) characteristics were extracted for each one between -1 V and 1 V.

After the electrical characterization, the working samples were connected inside an aluminium cage, used both to maintain the sample in the dark and as a Faraday cage, using silver paint and gold wires (Figure 2.3a) and were then ready to be characterized under X-Rays. A schematic of the measurement setup used to evaluate the X-Ray performance of each sample is reported in Figure 2.3b.

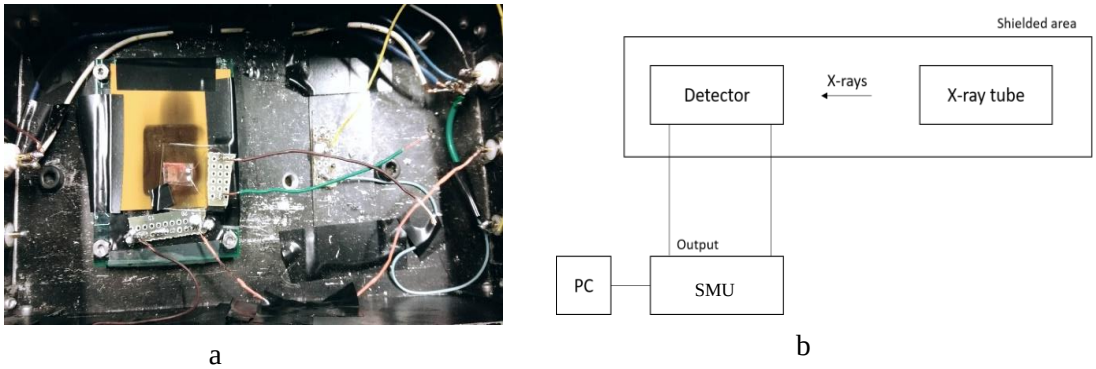

a b

Figure 2.3: a) one sample connected in the aluminium cage, used both to maintain the sample in the dark and as a Faraday cage and b) Schematic of the measurement setup used to evaluate the X-Ray detection performance.

The detector is placed in a shielded area at the distance of 23 cm from a molybdenum X-ray tube (PANalytical2, PW 2285/20), which operates at a voltage of 35 kV and at the current defined by the user (5 mA : 30 mA). The source meter unit (SMU) (Keithley 2614B) is connected to both the detector and a PC, allowing the user to control the system through the LabView software.

Samples are therefore subjected to a dose rate that depends on the X-ray tube's operation current. Figure 2.4 shows the dose rate-current calibration graph and Table 2.1 shows numerically the relation between the current and the dose rate at the distance of 23 cm from the beam source.

The parameters needed for the data acquisition are defined by the user through LabView interface. Under irradiation, the sample is kept in the dark, in air and at room temperature. To evaluate the response of the devices to X-ray in a comparable way, a standard procedure was chosen. The measurement was performed in order to obtain the current dynamical response (current versus time behaviour). In this case, during the acquisition, the X-ray beam is cyclically switched off for 60 seconds and then on for another 60 seconds, for 4 cycles. The bias voltage chosen for the measurement was 0.5 V to maintain the dark current as low as possible and minimize the electrical stress.

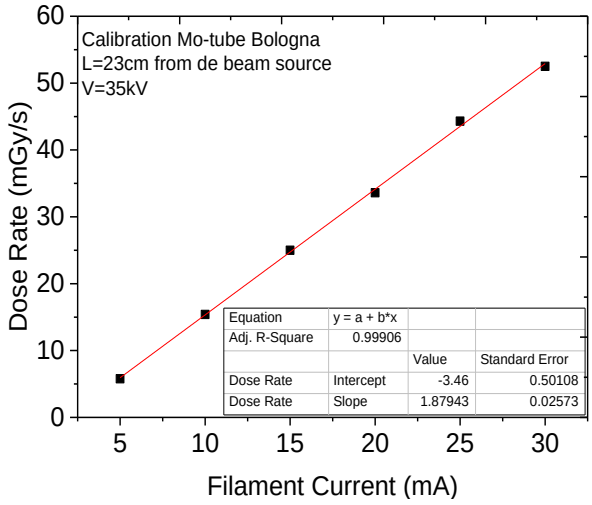

Figure 2.4: Calibration of the Mo-tube. Dose Rate vs Current.

Table 2.1: Relation between current and dose rate at the distance of 23 cm from de beam source.

Filament Current (mA)	Dose Rate (mGy/s)
30	52.5
25	44.3
20	33.6
15	25.0
10	15.4
5	5.8

After the X-ray characterization, it was conducted a study on the thin film crystallization structure and its influence on the detector performance. For this purpose an atomic force microscope (AFM) in non-contact mode and an optical microscope were used.

3 Characterization of TIPS and TIPGe based detectors

In this chapter the results of the TIPS-pentacene and TIPGe-pentacene based detectors will be presented and discussed. The chapter is divided in three parts, where the first two correspond to the two different substrates tested (PEN and glass) and the final one is composed by a short summary.

3.1 PEN substrate

Five devices were fabricated in a PEN substrate. Three of them with the TIPS molecule and two with the TIPGe. The data presented in this subsection is related to the best detector achieved in each case in terms of sensitivity.

3.1.1 Electrical Characterization

The first step in the characterization of any kind of electrical device is, in fact, the analysis of its electrical behaviour. In Figure 3.1, the I-V characteristics, between -1 V and 1 V, of the best device in terms of sensitivity of TIPS and TIPGe on PEN are reported. The current achieved at 1 V for the TIPS device is 7 nA and for the TIPGe device is 31 nA, which means that the TIPGe device reaches a higher current, as expected.

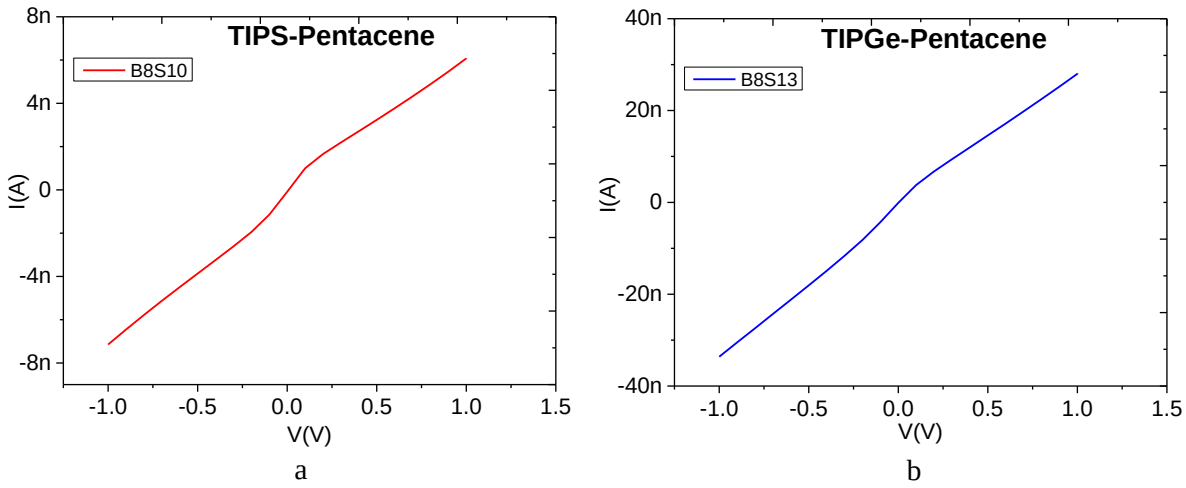

Figure 3.1: I-V characteristic of a) TIPS-pentacene detector and b) TIPGe-pentacene detector on PEN.

In addition, the sheet resistivity, of each device was calculated, mostly for the comparison with the values acquired for the devices with the PET substrate given that they do not have the same dimensions.

Using the centre-to-centre distance along the current path (L) as the sample length and the distance between voltage probes perpendicular to the current path as the sample width (W) [37], the sheet resistivity $\rho_{\square}$ can be calculated by the following equation (1):

$$\rho\square = \frac{R \times W}{L} \quad (1),$$

where the resistance (R) is calculated as R=V/I, after the ohm's law, at 1 V.

In this case, the TIPS device had a sheet resistivity of 1.1×10^{12} Ω□ while the TIPGe device had 2.2×10^{11} Ω□. This is high, which goes accordingly to the requirement of a good detector. Nevertheless, there should be a compromise in this parameter because the resistivity cannot be high to the point where there is no current in the device (even in the exposure). We can conclude that in comparison, the TIPGe device should conduct current better than the TIPS one. So far, it is not well known if there is or what is the influence of this parameter in the X-Ray response.

3.1.2 X-Ray Characterization

The dynamical behaviour to X-Ray exposure of the current at different dose rates related to the TIPS detector is presented in Figure 3.2. It is possible to see that the current is not high being in the few nA, which is translated into the low sensitivity of the device, 7.5 nC/Gy (Figure 3.2b). The sensitivity of the device, in this case, is measured as the slope of the line that relates the average of the photocurrent, having in consideration the 4 cycles OFF/ON of radiation exposure, with the respective dose rate (∂I/∂D) [1]. The photocurrent, as the name implies, is the current caused by exposure to radiation.

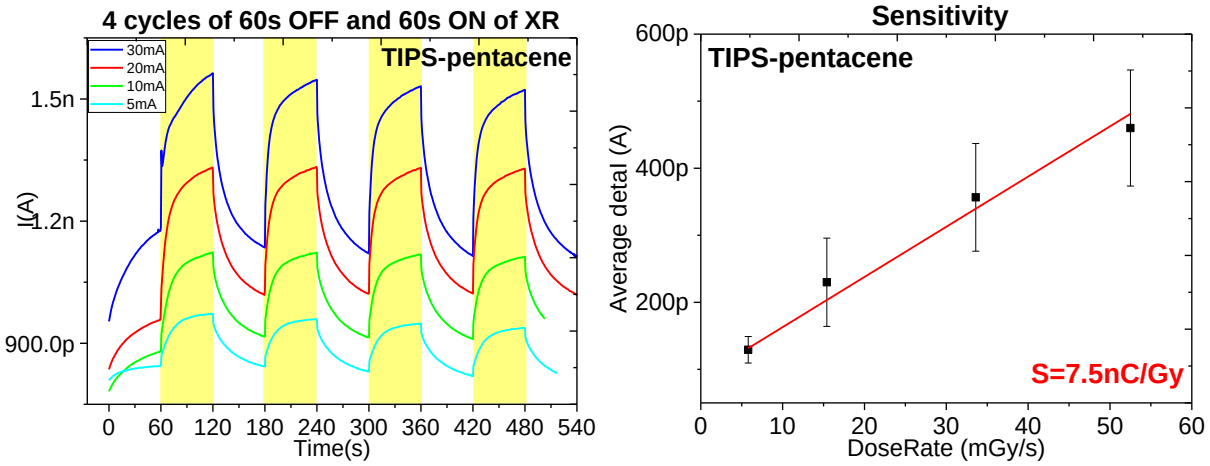

a b

Figure 3.2: a) Dynamical behaviour of a TIPS detector on PEN at different dose rates and b) Photocurrent vs Dose Rate of the same detector.

In the literature, the highest experimental sensitivity, with the TIPS molecule, reported was 180 nC/Gy and was obtained for long exposure times and low dose rates with the PET substrate [1]. That value is, obviously, not comparable with the one reported here on PEN. Nevertheless, that high value was obtained after many batches performed at UNIBO in which there were detectors with high and low sensitivities as well as devices not working at all. Therefore, there are some problems with reproducibility with this molecule TIPS on PET and a more controlled fabrication method is desired to reduce

sample variability. For this reason, it does not make sense to compare the results reported here with PEN with the one reported in the literature for PET because the sample population is too different.

Even with a low sensitivity, from the dynamical response of the device, it is noticeable that, even though there is only a difference of few nA with the increasing of the dose rate, there is no electrical stress involved during each measurement because the maximum and minimum peaks of the current in each cycle of exposure are always similar. This is a very positive point given that it shows the stability of the device. Nevertheless, it is also noticeable that the dark current is not the same in each dose rate which proves that some bias stress is there at least between the measurements. The first dose to be tried was the highest one, the one equivalent to the 30mA of filament current (52.5 mGy/s), because it has the highest dark current. The dose rate was, then, decreased to the one equivalent to 20mA (33.6 mGy/s) and so on until the lowest one (5.8 mGy/s). The order should not make a difference, but due to the bias stress effect it is preferable to start with the highest dose making sure that the measurement of the photocurrent is as little affected by the bias stress phenomenon as possible.

The response signal, which is the photocurrent, increases exponentially and it does not seem to reach saturation. It is important to point out that the photocurrent increases linearly with the dose rate which is another positive point with these devices as it stands for their reliability.

As stated before, the TIPGe molecule should give better results as an X-Ray detector because of the higher Z number of germanium. This is proven by the dynamical behaviour of the detector at different dose rates, presented in Figure 3.3a, being visible a higher step in the current with the increasing of the dose rate. This is translated into the higher sensitivity achieved by this device, reaching 29.6 nC/Gy.

The analysis is very similar to the previous one. The photocurrent has an even more linear increase with the dose rate than the TIPS device and it is possible to see some electrical stress, especially with the highest dose (52.5 mGy/s), but still not significant. The response signal also increases exponentially and it does not reach saturation.

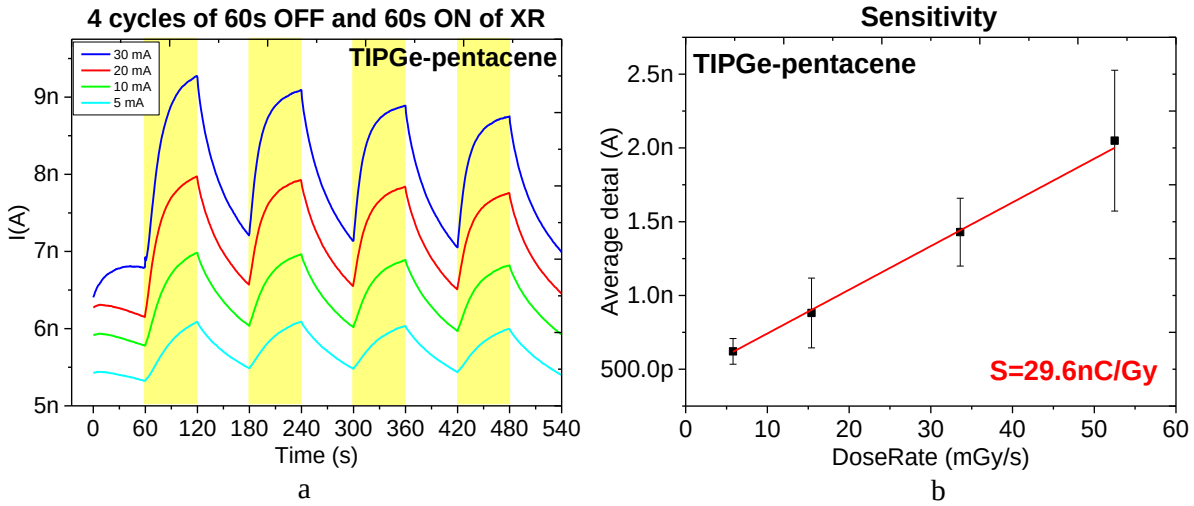

Figure 3.3: a) Dynamical behaviour of a TIPGe detector on PEN at different dose rates and b) Photocurrent vs Dose Rate of the same detector.

Another important parameter that was calculated was the signal to noise ratio (S/N), which is the ratio between the X-Ray induced photocurrent and the current in dark [1]. For the TIPS based device the signal to noise ratio for the highest dose was 4.1×10^{-1} while for the TIPGe detector was 2.9×10^{-1} for

the same dose. These values are high which is very good because it means that the dark current is low when compared with the photocurrent.

In Table 3.1, the maximum current and sensitivity of all the detectors fabricated with the TIPS and TIPGe molecules on PEN are reported. The values in red are those that correspond to the presented graphs and, therefore to the best detectors.

With the TIPS molecule, out of the three samples manufactured, two of them presented the same sensitivity (4.1 nC/Gy) and the highest current at 1 V (7 nA) corresponds to the highest sensitivity (7.5 nC/Gy). With the TIPGe molecule, the two devices are quite similar. It is possible to conclude that even if the sensitivity is low, the devices are reproducible and reliable given that: there is no discharge, there is no significant electrical stress, the photocurrent is constant with the increasing of the cycle of exposure and increases in a linear way with the dose rate. It is important to note that the samples with the same molecule have similar sensitivities which proves once again the reproducibility of the devices.

Table 3.1: Sensitivity and maximum current of all the devices fabricated with TIPS and TIPGe on PEN.

Molecule	Sample	Imax (1V) (nA)	Sensitivity (St)(nC/Gy)
TIPS	S10	7	7.5
	S11	5	4.1
	S12	3	4.1
TIPGe	S13	31	29.6
	S14	34	27.9

3.1.3 Optical microscope

The microscope pictures show good crystallization with aligned crystals, Figure 3.4. In comparison, the TIPGe thin film seems to crystalize better because the individual crystals are clear and aligned, more than on the TIPS film. The channel is full of crystals in both cases, which in theory is desirable since without it there would not be a collection of the charges in the electrodes.

An important point to note is that, although the images shown in Figure 3.4 translate a small portion of the detector, it has been found that they represent well the entire active area of the detector. Not only that, but different images of different devices manufactured with the same molecule are similar. This goes accordingly to the reproducibility already mentioned of this type of films.

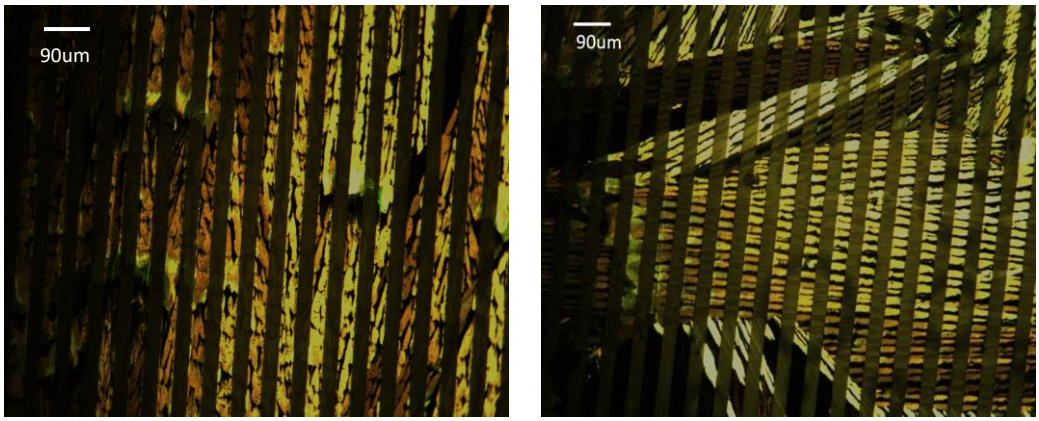

a b

Figure 3.4: Microscope pictures of a) TIPS based detector and b) TIPGe based detector on PEN.

3.2 Glass substrate

Eight devices were fabricated in a glass substrate. Four of them with the TIPS molecule and another four with the TIPGe. 80% of the devices worked immediately and the two that did not work were in short-circuit electrically. The data presented in this subsection is related to the best detector achieved in each case in terms of sensitivity.

3.2.1 Electrical characterization

The I-V curves of the best device of TIPS and TIPGe on glass are presented in Figure 3.5. The current achieved at 1 V for the TIPS device is 160 nA and for the TIPGe device is 195 nA. These values are higher than the ones achieved with the PEN substrate. The form of the curves is similar to the one presented for the PEN (Figure 3.1), meaning that the not completely linear electrical behaviour is connected to the fabrication of the substrates having into account that both the PEN and the glass have the same dimensions and were manufactured in the same place (CENIMAT). The TIPGe device continues to have a higher current, as expected.

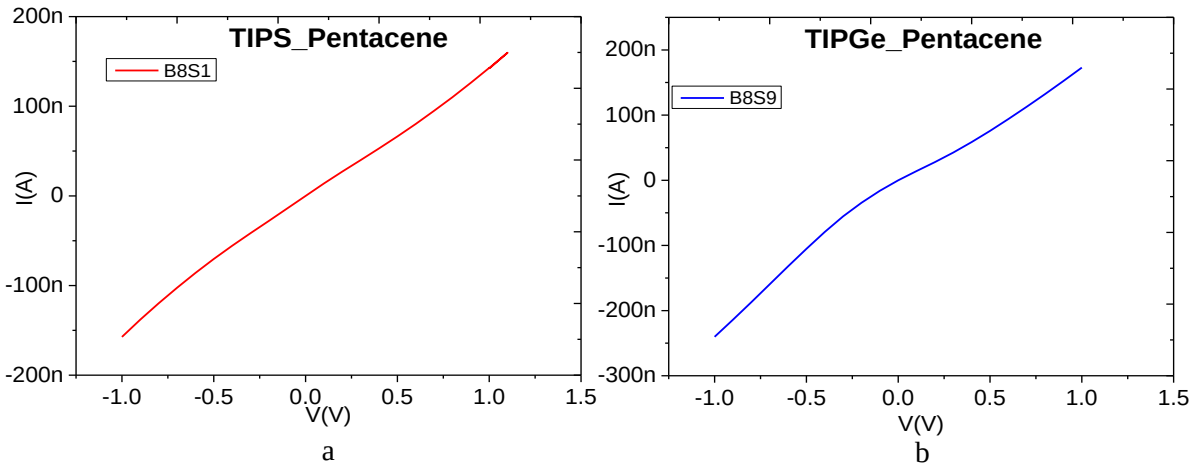

a b

Figure 3.5: I-V characteristic of a) TIPS-pentacene detector and b) TIPGe-pentacene detector on Glass.

The sheet resistivity was, once more, calculated for both devices and it was found that for this type of detectors they were both very similar: the TIPS detector had 4.3×10^{10} Ω□ and the TIPGe one had 3.5×10^{10}Ω□. These values are not as high as the ones reported for PEN, which is not desirable but, as it will be seen by the X-Ray characterization, this parameter is not as significant as others when it comes to achieving a high sensitivity.

3.2.2 X-Ray Characterization

In Figure 3.6, the X-Ray characterization of the TIPS based device on a glass substrate is presented. The sensitivity achieved is 7.9 nC/Gy, which is very close than the one on the PEN substrate. Nevertheless, there are some differences.

Firstly, the electrical stress is more obvious: the highest dose was the one tested initially, and it is noticeable that during the first exposure there is a photocurrent of roughly 4 nA that, not only does not stay constant throughout the rest of the exposures but actually decreases. The dark current also decreases with time. All of this is translated into a signal to noise ratio of 2.5×10^{-1}.

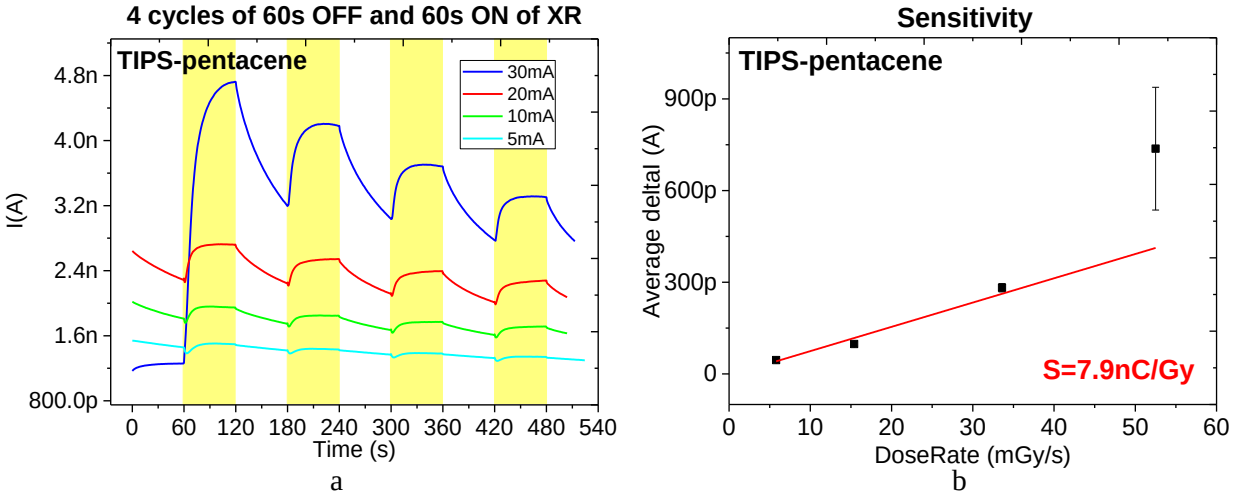

Figure 3.6: a) Dynamical behaviour of a TIPS detector on glass at different dose rates and b) Photocurrent vs Dose Rate of the same detector.

The growth of the photocurrent with the dose rate is linear until the 33.6 mGy/s, having a big increase with the highest dose (52.5 mGy/s). This could also be a consequence of the drift of the current. The response signal follows an exponential trend but in this case the photocurrent reaches a saturation which means that with these devices, 60 s of exposure are not necessary, and the result would be the same with a lower time of exposure (30 s for example) which is always preferable because it would reduce the bias stress effect.

Surprisingly, the TIPGe based device on glass had a very different behaviour than the TIPS one as it is possible to confer in Figure 3.7. The major difference of this graph (Figure 3.7a) is the current, which is higher, in this case going up to the 35 nA. This means that there is a larger dark current in this device, which is not desirable. In fact, a perfect detector would have no current in the dark, and then, when exposed to the radiation would have a big photocurrent. In the previous analysed devices, the dark current was smaller but so was the photocurrent. In this case, the photocurrent reaches 8 nA which is really high in comparison with the other detectors. This means that having the lowest dark current

possible should not be the priority when it comes to achieving a high performance detector but the relation between the dark current and the photocurrent, a compromise between the two needs to be found.

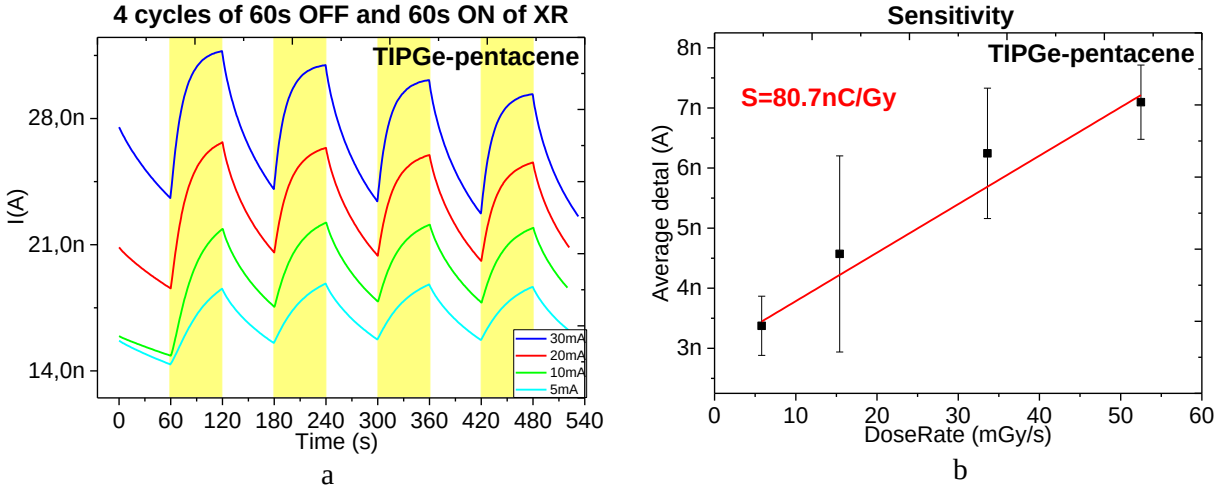

Figure 3.7: a) Dynamical behaviour of a TIPGe detector on glass at different dose rates and b) Photocurrent vs Dose Rate of the same detector.

With the TIPGe based detector on glass, the photocurrent seems to grow in a linear way with the dose rate even with an error more considerable. The sensitivity of this detector is 80.7 nC/Gy, being really high comparing with the other devices. The signal to noise ratio is 3.1×10^{-1} at 30 mA, higher than the detector with TIPS on glass which, given the much higher sensitivity achieved, is normal.

When it comes to the bias stress effect, it is slightly there with the highest dose rate but it is not significant, and it disappears almost completely with the other doses. The signal increases exponential, similarly to the other analysed devices, but it does not reach saturation and it would in fact benefit from a longer exposure time because the photocurrent is still significantly increasing after the 60 s of each cycle of exposure.

In Table 3.2, it is possible to find a summary of the sensitivity and the maximum current reached by all the devices that worked. Again, the values in red are the ones that correspond to the graphs reported in this section.

First of all, based on this set of samples, the current at 1V does not seem to be directly connected to the sensitivity of the device. Sample S7 had a maximum current at 1 V of 368 nA and its sensitivity was 53.3 nC/Gy which is lower than the one reached by sample S9 of 80.7 nC/Gy, that had a maximum current of 195 nA. Not only that, sample S4 had a maximum current of 57 nA, which is roughly in the middle of the maximum current of sample S2 (103 nA) and S3 (18 nA), nevertheless its sensitivity is of 6.6 nC/Gy, being higher than both the sensitivities achieved by S2 and S3.

Both the TIPGe based detectors have high sensitivities. The glass substrate with this molecule should give the best performing X-Ray detector.

Table 3.2: Sensitivity and maximum current of all the devices fabricated with TIPS and TIPGe on glass.

Molecule	Sample	Imax (1V) (nA)	Sensitivity (St)(nC/Gy)
TIPS	S1	160	7.9
	S2	103	3.1
	S3	18	3.4
	S4	57	6.6
TIPGe	S7	368	53.3
	S9	195	80.7

3.2.3 Optical microscope

In Figure 3.8, the microscope pictures of the TIPS and TIPGe based detectors on glass can be found. The thin films demonstrate, once again, good crystallization with aligned crystals. Comparing the two, the TIPGe thin film seems to have smaller crystals and slightly more individualized than the TIPS film. The channel is, once more, full of crystals in both cases.

At this point, given that the TIPGe thin film always has smaller, more aligned and uniform crystals than the TIPS one, it is possible to conclude that there is a relation with the mobility of the carriers and therefore the sensitivity of the device. This goes accordingly to the literature that says the hole mobility in acene molecules is largely dependent on crystal orientation and crystal quality, i.e., the size of the single crystal domains, the presence of cracks and the crystal thickness [38]. Therefore, one possible explanation for the higher sensitivity with the TIPGe based device, other than the Z number of germanium, is the crystal quality observed in the thin film.

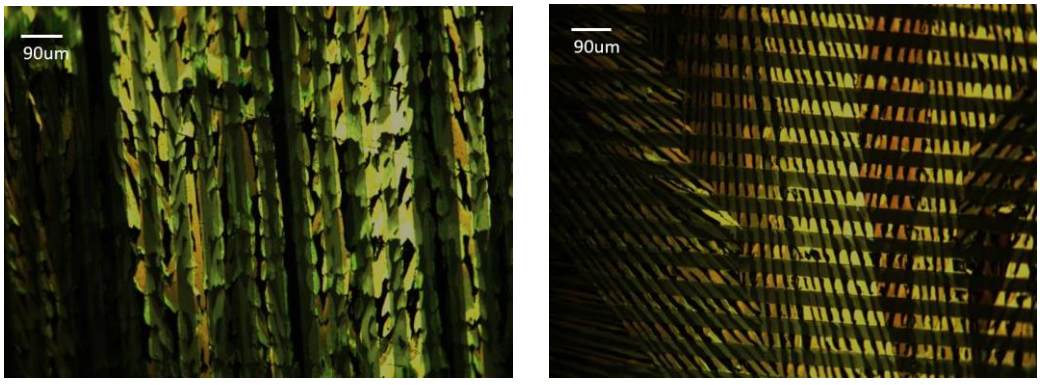

a b

Figure 3.8: Microscope pictures of a) TIPS based detector and b) TIPGe based detector on glass.

3.3 Summary

In Table 3.3, a summary of the most important parameters of the best TIPS and TIPGe based detectors in both substrates tested is presented. One of the first and most important conclusions possible to take is that, in fact, the TIPGe based detector is always better than the TIPS based device in all the parameters. The sensitivity per active area was calculated so the substrates could later be compared with the devices of the following chapter having into consideration that PET does not have the same dimensions as PEN and glass.

Table 3.3: Summary of the most important parameters of the best detector based on TIPS and TIPGe on PEN and glass.

Substrate	Molecule	Imax (1V) (nA)	Sheet Resistivity (Ω□)	Total Sensitivity (St)(nC/Gy)	St/ActiveArea (nC/Gy.cm^2)	(S/N) at 30 mA
PEN	TIPS	7	1.1×10^{12}	7.5	43	4.1×10^{-1}
	TIPGe	31	2.2×10^{11}	29.6	170	2.9×10^{-1}
Glass	TIPS	160	4.3×10^{10}	7.9	46	2.5×10^{-1}
	TIPGe	195	3.5×10^{10}	80.7	461	3.1×10^{-1}

As explained in the literature, achieving high sensitivities with these molecules TIPS and TIPGe is related to trap states. The theory is that, under X-Ray irradiation, when the additional electrons and holes are generated, the holes drift along the electric field and reach the collecting electrode while electrons remain trapped in deep trap states and act as “doping centers”. Therefore, to guarantee charge neutrality, holes are continuously emitted from the injecting electrode. Hence, for each electron-hole pair created, more than one hole contributes to the photocurrent, causing an increase in the material conductance and a photoconductive gain [1]. Given that this particular PEN is a Q65 teonex , which has an extremely smooth surface [39], it is possible that it does not have many structural defects and therefore less trap states to the electrons which could lead to a lower sensitivity measured. However, with the PEN substrate, there is a very good adhesion to the organic molecules proved by the microscope pictures that show really good quality crystals which is translated in reliable and reproducible devices.

The glass substrate with the TIPGe would be the best one because it combines a high sensitivity with a reliable device. Nevertheless, glass is not a flexible substrate and is therefore not suitable for many of the applications in interest for example wearable health diagnostic applications like a personal dosimetry.

4 Characterization of diF TES ADT and diF TEG ADT based detectors

The results of the diF TES ADT and diF TEG ADT based detectors will be reported and commented in this chapter. Analogously to the previous chapter, is divided in four parts, the first three correspond to the three different substrates tested (PET, PEN and glass) and the final one is composed by a brief summary.

4.1 PET substrate

Ten samples based on diF TES ADT and diF TEG ADT were fabricated on a PET substrate, five of each molecule. 70% of the detectors worked, all the devices of diF TES ADT and two of diF TEG ADT. All of them presented a big discharge that will be explained, but with the diF TEG ADT samples this phenomenon took longer. With the diF TES ADT, the samples were left exposed to the radiation for 1 hour and after that started to respond properly. With the second molecule, the two samples that worked were left exposed for more than 1 hour, the other three devices never left that state of discharge. The data presented in this subsection is related to the best detector achieved in each case in terms of sensitivity.

4.1.1 Electrical Characterization

The electrical characterization of the best device of each molecule is presented in Figure 4.1. The current in diF TEG ADT is 2 times higher reaching, at 1 V, 2.9 µA, while diF TES ADT reaches 1.3 µA at the same voltage. This goes accordingly to the expected given the higher Z number of germanium compared to silicon, as explained before.

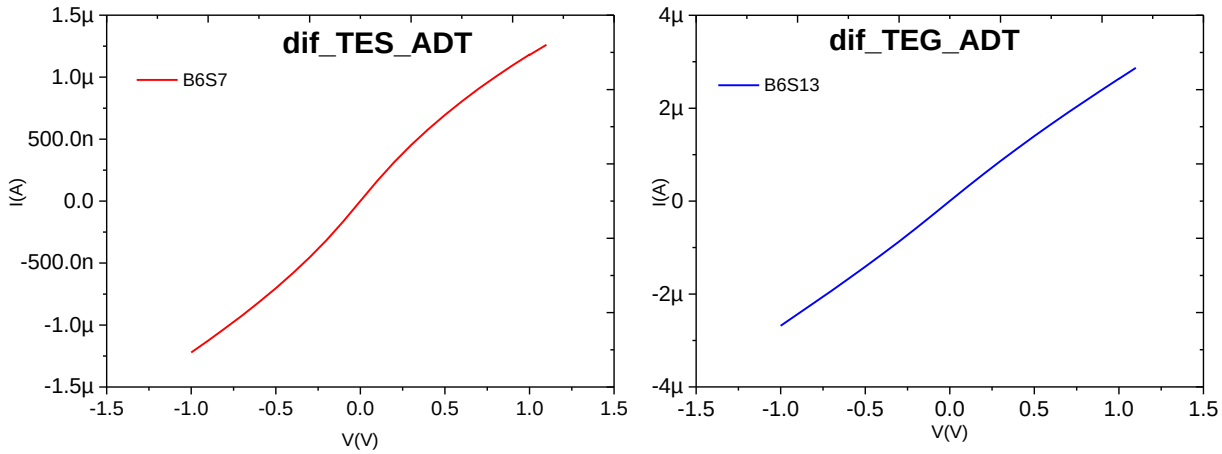

a b

Figure 4.1: I-V characteristic of a) diF TES ADT detector and b) diF TEG ADT detector on PET.

The sheet resistivity was calculated for both devices, being obtained a value of $1.3 \times 10^9\,\Omega\square$ and $5.8 \times 10^8\,\Omega\square$ for diF TES ADT and diF TEG ADT, respectively. The diF TEG ADT device should conduct current better but, then again, there has to be a compromise here because a good detector should have a good resistivity in order to have a low dark current and therefore a large signal to noise ratio.

4.1.2 X-Ray Characterization

As stated before, all of these samples presented a strong discharge of the current during the first exposure to X-rays. This is probably due to trap states in the interfaces that essentially trap the charges and prevent them from moving, causing a continued decrease in the current. These traps can be formed by structural defects (resulting in local positional or energetical disorder), dipoles, excimers, or guest molecules (impurities or dopants) or even due to the oxygen in the air that is adsorbed on PET and can trap electrons because of their high electron affinity and act as additional surface states [40][41]. In Figure 4.2, it is possible to find an example of this phenomenon and it is visible that with the exposure to X-Ray, this is even more intensified which is easily explained by the fact that the radiation gives energy to the charges and therefore they try to move and become trapped, not reaching the electrodes where they were supposed to be collected.

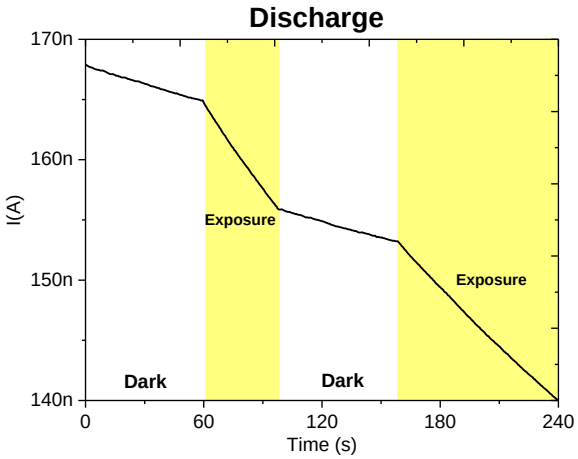

Figure 4.2: Discharge process in a diF TES ADT based detector on PET.

It has been proven that the detrapping of charge carriers may be induced by molecular relaxations. The relaxation effect may be caused by a redistribution of energy among the nuclear, electronic, vibrational, and rotational energy states of the atoms and molecules that constitute the system. This effect may facilitate the inter–site hopping of charge carriers by lowering the potential barriers of the trapping sites or by decreasing the distance between the neighbouring localized sites [40] [42]. So, all the devices that presented discharge were left exposed to radiation for one hour in order to try to achieve this relaxation state. After that, the detector is left resting for 5 minutes before attempting a new measurement. It was found that this worked well and all of the devices based on diF TES ADT begun to respond as expected to the X-Ray irradiation.

In Figure 4.3, the dynamical behaviour, after the discharge, of the best diF TES ADT detector at different dose rates is reported. It is possible to see that there is a response to the X-Ray. Nevertheless, the bias stress is present and the dark current is high and so it is not easy to properly evaluate and

compare the response at different dose rates. For that reason, it is needed a normalization of the current. This consists in subtracting the dark current from the total current and thus obtaining a graph that only portrays the photocurrent and where, ideally, in the period of time when there is no radiation exposure there would be no current. This is illustrated in Figure 4.4a.

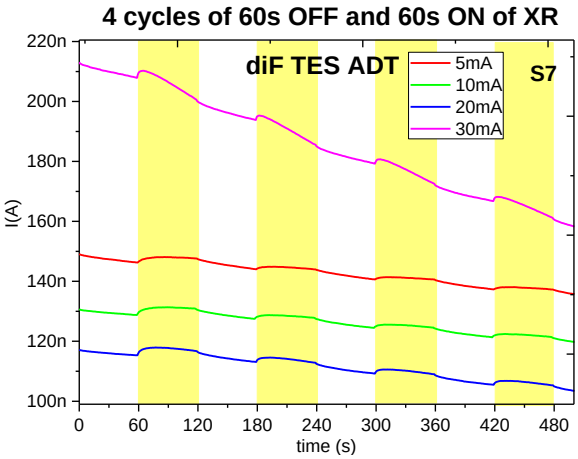

Figure 4.3: Dynamical behaviour of the best detector based on diF TES ADT on PET.

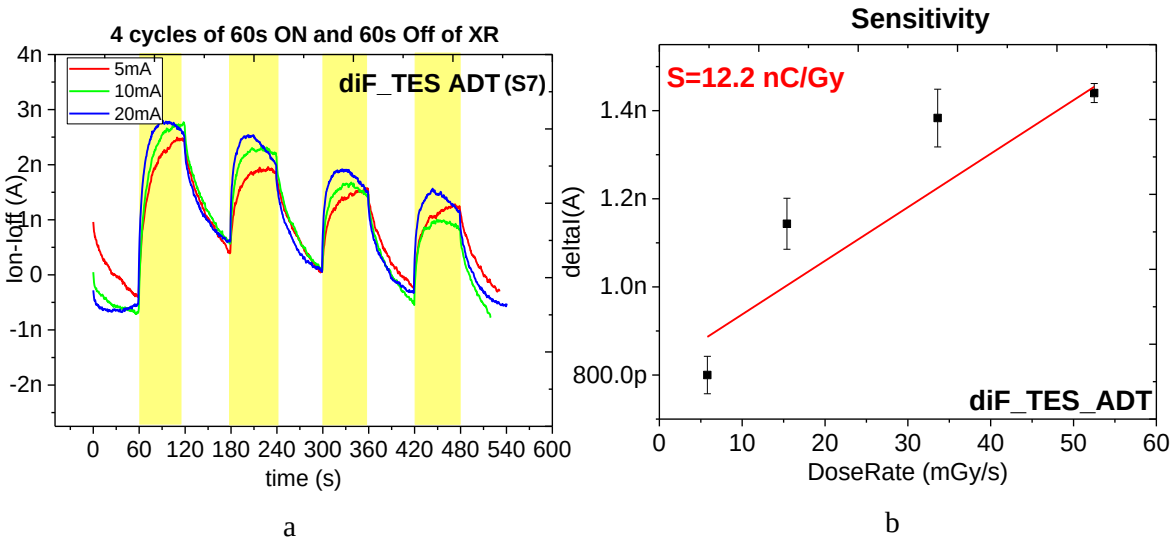

a b

Figure 4.4: a) Normalized graph of the dynamical behaviour of a diF TES ADT detector on PET at different dose rates and b) Photocurrent vs Dose Rate of the same detector.

The current at the highest dose (52.5 mGy/s) was not possible to normalize in a way that could translate the reality, the dark current shifted too much during the experience due to the bias stress suffered. For that reason, this dose is not illustrated in the graph of Figure 4.4.

The photocurrent does not have a linear increase with the dose rate being, in this case, more like an exponential increase. The sensitivity of the detector is, in this case, 12.2 nC/Gy. This value is not as high as it was expected and given the high dark current of the device it is possible to conclude that this combination of molecule on PET with the drop casting does not present the desirable results. All of this is translated into the signal to noise ratio that is low being, at 30 mA, 8.0×10^{-3}.

It is possible to see that with the highest dose presented (33.6 mGy/s) the velocity of the signal is quite fast given that the peak of the current is obtained roughly after 20 seconds of exposure and after that it starts to slowly decrease again. This is no longer the case with the smallest doses (15.4 and 5.8 mGy/s): here the current continues to grow exponentially throughout the 60 seconds of exposure never reaching a saturating value. This difference in the response times is explained by the fact that with the highest doses, there is a bigger quantity of photons that will interact with the molecule and create more electron-hole pairs per second that will reach the electrodes faster while with the smallest doses, the quantity of photons per second is not enough to excite all the electrons at once and so the photocurrent continues to increase never reaching a steady value.

In Figure 4.5, the dynamical behaviour of the normalized current at different dose rates of the best diF TEG ADT based detector on PET is presented. The sensitivity is lower than the device based on diF TES ADT, this does not go accordingly to the expected given the higher Z number of germanium. Also, the photocurrent does not have a linear growth with the dose rate and it actually decreases with the highest dose. This could be explained with the discharge process that being much longer for diF TEG ADT than for diF TES ADT, induces a larger decrease in the current, even without X-Ray, due to the electrical stress, which results in a lower calculated sensitivity. Nevertheless, it is important to point out that this batch was the first one at UNIBO with this type of working devices and it is necessary a better understanding of the discharge phenomenon and how to control it in order to obtain the desirable results.

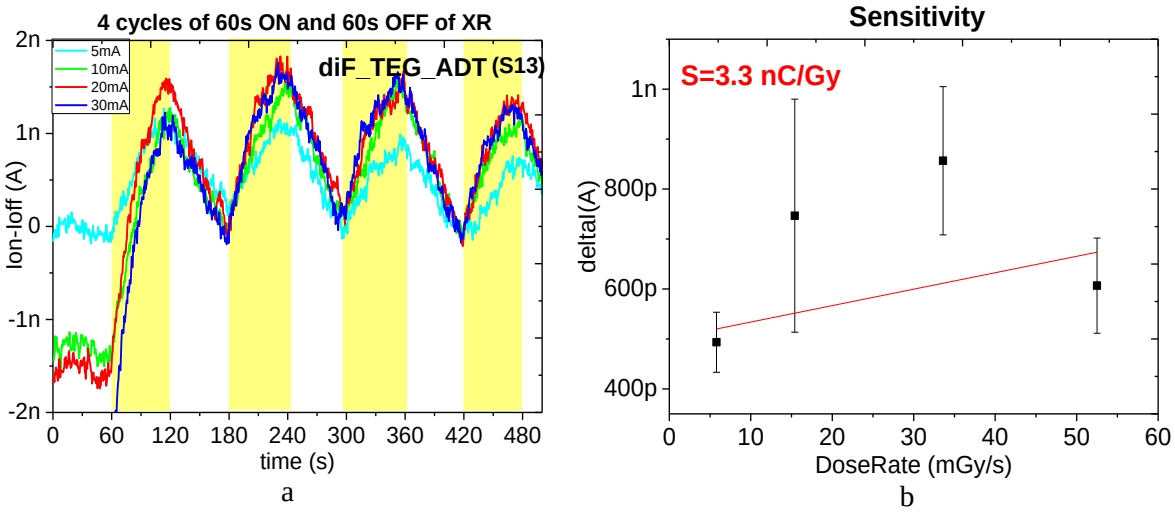

Figure 4.5: a) Normalized graph of the dynamical behaviour of a diF TEG ADT detector on PET at different dose rates and b) Photocurrent vs Dose Rate of the same detector.

The response signal is linear as it continues to increase until the end of the 60 s of exposure never reaching a constant value. Once again, it would be interesting to check for how long the photocurrent would continue to increase. Examining the curves, it is very clear that there is a lot of noise in this measurement. The dark current is high, being roughly 485 nA in the highest dose and the signal to noise ratio is, therefore, low, 1.3×10^{-3}.

4.1.3 Atomic Force Microscope

With this batch, due to the fact that the sensitivity results were not as expected, it was decided to use an Atomic force Microscope (AFM), to image the topography of the samples, which is possible with AFM with atomic resolution [43].

In the AFM the sample is scanned by a tip, which is mounted to a cantilever spring. While scanning, the force between the tip and the sample is measured by monitoring the deflection of the cantilever. A topographic image of the sample is obtained by plotting the deflection of the cantilever versus its position on the sample. It is also possible to plot the height position of the translation stage. [43]. This would give us the height of the crystals which could be related to the conductivity of the devices and therefore their performance as radiation detectors.

First of all, the images taken with the AFM in non-contact mode, of two devices based on diF TES ADT (S7 and S8) were compared and can be found in Figure 4.6. It seems that S7, the sample with the highest sensitivity, has thinner crystals, but the thickness of the crystals in sample S8 is bigger. From the evaluation of all the samples it was found that the highest sensitivity is therefore related to the thinner grains but in a dense aligned form. In all of the dif TES ADT samples, one can see that the grains are in a long structure and in a uniform distribution.

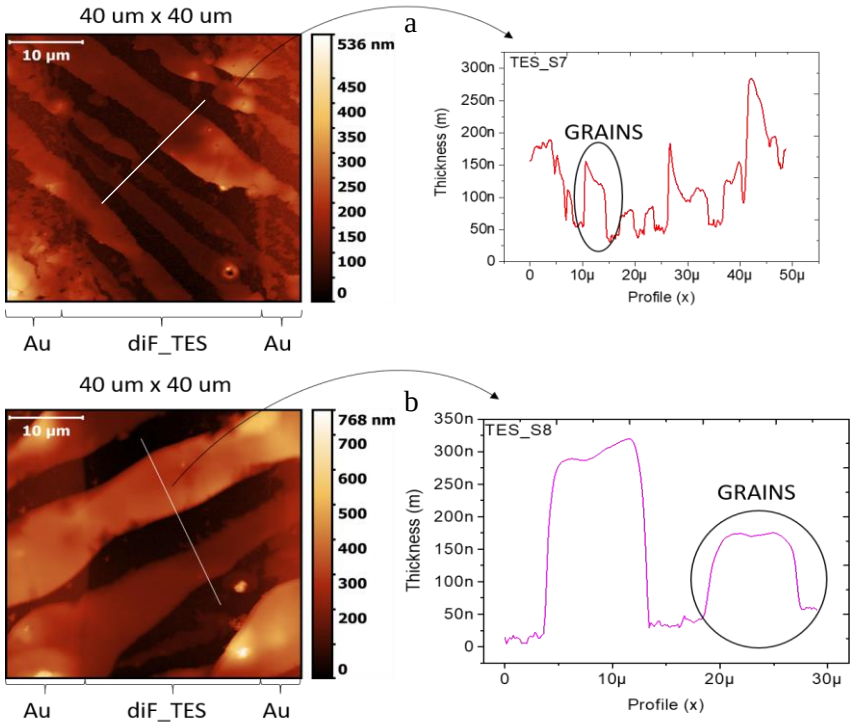

Figure 4.6: AFM images and film thickness profile of a) sample S7 and b) sample S8 (both diF TES ADT).

In Figure 4.7, the AFM image and the thin film thickness profile of the best device based on diF TEG ADT on the PET substrate is presented. In comparison with the previous samples, it has thicker crystals. But, once again, this does not seem to have a big influence on the sensitivity when all the samples are taken into consideration.

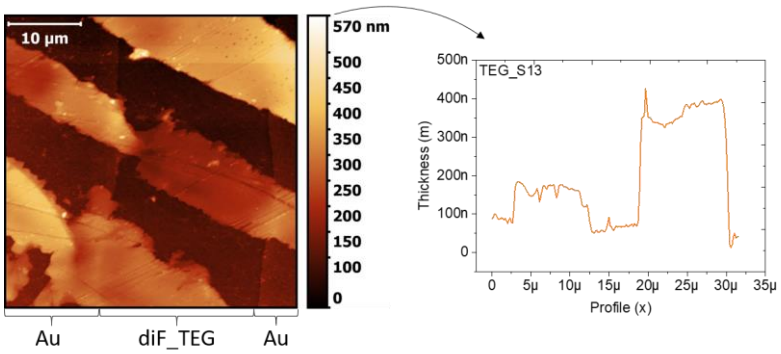

Figure 4.7: AFM image and thickness profile of sample S13 (diF TEG ADT).

In Table 4.1 is presented a summary of the sensitivity, the current at 1 V and the thickness of the bigger crystal of all the detectors that, after the discharge, responded to the exposure of the radiation. The values in red correspond to the devices chosen to be presented in this subsection, which means the best ones in terms of sensitivity.

Based on this batch of samples, the maximum current and therefore the conductivity of TEG is greater than the one of TES, one order of magnitude more. In general, the devices which present a higher current within the same molecule show also the greatest sensitivity, yet, not in a proportional way.

The best device based on diF TES ADT presents a sensitivity that is out of the average one, comparing with the other detectors. This would be difficult to explain given that all the samples were fabricated in the same conditions. However, it was clarified by the comparison of the AFM images that showed that S7 had, not only a lot more crystals, but also a lot more active area of the device covered by the semiconducting thin film. It appears that the thickness of the crystals is not an important parameter for the performance of the detector, both in terms of sensitivity and electrical performance.

Table 4.1: Sensitivity, maximum current and thickness of the bigger crystal of all the detectors based on diF TES ADT and diF TEG ADT on PET.

Molecule	**Sample**	**Imax (1V) (nA)**	**Sensitivity (St)(nC/Gy)**	**Thickness (nm)**
TES	S3	169	2.1	300
	S4	1210	2.3	270
	S7	**1260**	**12.2**	**200**
	S8	116	1.4	290
	S10	125	3.4	940
TEG	**S13**	**2870**	**3.3**	**400**
	S14	4150	2.3	550

In Figure 4.8, it is possible to compare both the thin films of diF TES ADT and diF TEG ADT. The TEG samples has fewer grains, larger, not long and thicker crystals. This could be related to the longer discharge process. The most important finding with the AFM study was that there is obviously a general problem of adhesion: the organic molecules do not crystallize well on the PET substrate, especially on the channel as it was hard to find an area of the channel with crystals. Moreover, there were areas within the same sample with many crystals but also areas without any. For further conclusions, it would be important to fabricate these detectors in a transistor structure to obtain more detailed information about the parameters which characterize a good radiation detector, for example the mobility of the carriers.

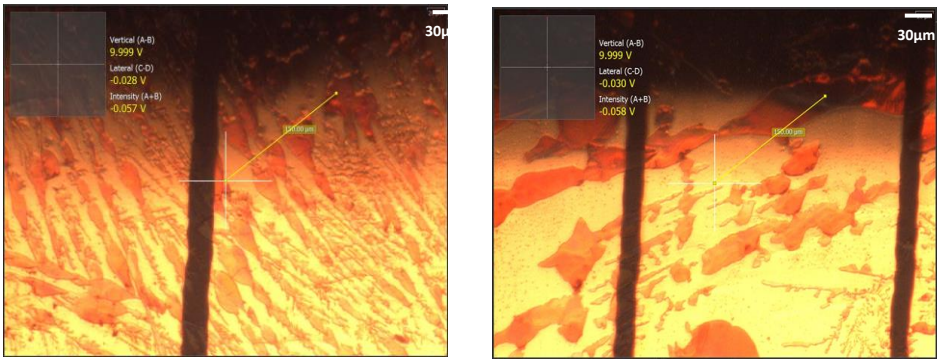

a b

Figure 4.8: a) diF TES ADT and b) diF TEG ADT thin film images taken by the optical microscope of the AFM.

4.2 PEN substrate

Six detectors were fabricated on a PEN substrate. Three of them with the diF TES ADT molecule and three with the diF TEG ADT. All of the devices worked right away with no discharge. The data presented in this subsection in related to the best detector achieved in each case in terms of sensitivity.

4.2.1 Electrical Characterization

The I-V curves of the best device in terms of sensitivity of diF TES ADT and diF TEG ADT on the PEN substrate are reported in Figure 4.9. The current achieved at 1 V for the diF TES ADT device is 8 nA and for the diF TEG ADT device is 970 nA. The diF TEG ADT device continues to have a higher current as expected. Again, with this substrate is observed a behaviour not completely linear, especially with the diF TES ADT, probably due to a problem of the substrate fabrication.

The diF TES ADT based detector had a sheet resistivity of 9.1×10^{11} Ω□ and the diF TEG ADT device had 7.1×10^{9} Ω□ which goes, once again, accordingly to the expected. The molecule with the germanium should conduct better.

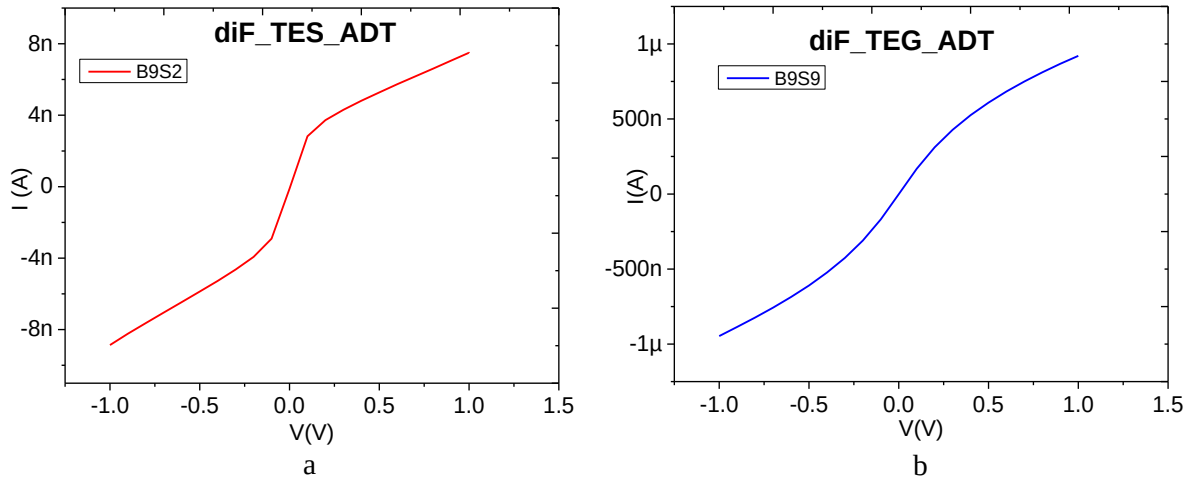

Figure 4.9: I-V characteristic of a) diF TES ADT detector and b) diF TEG ADT detector on PEN.

4.2.2 X-Ray Characterization

The dynamical behaviour to X-Ray exposure of the best diF TES ADT detector on PEN at different dose rates is presented in Figure 4.10. Once again, the current is not high being in the few nA while the photocurrent is in the pA. This is translated into the low sensitivity of the device, 13.3 nC/Gy, Figure 4.10.

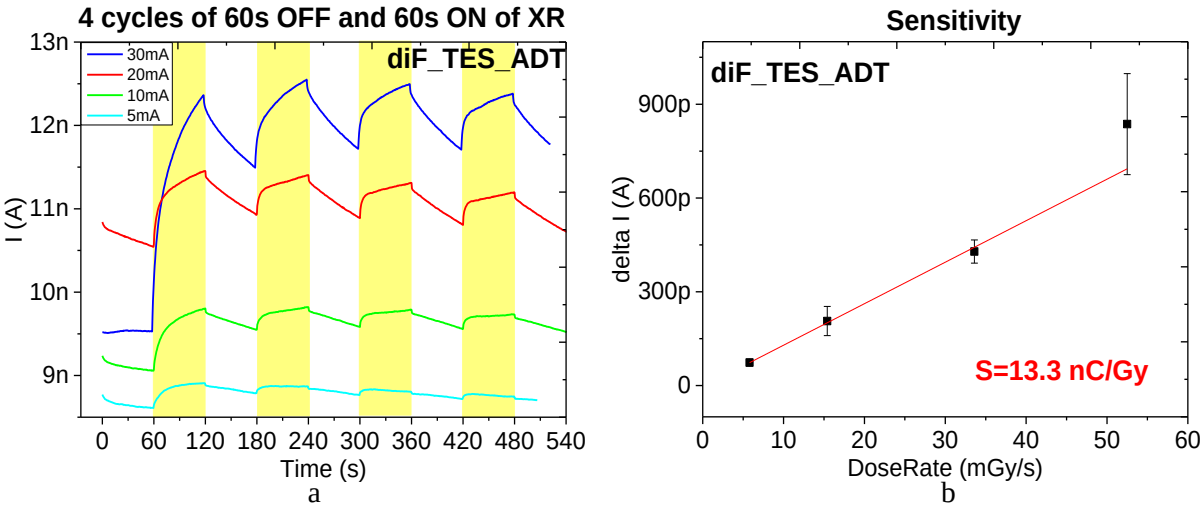

Figure 4.10: a) Dynamical behaviour of the best diF TES ADT detector on PEN at different dose rates and b) Photocurrent vs Dose Rate of the same detector.

Analysing the curves, it is possible to conclude that there is not a lot of electrical stress because there is no drift of the current with time which means that the device is very stable. The response signal increases exponential, but it does not reach saturation and it would definitely benefit from a longer exposure time because the photocurrent seems to be still significantly increasing after the 60 s of each cycle of exposure especially for the highest dose rate. The photocurrent increases in a linear way with the dose rate. Finally, this detector presents a low dark current which is desirable, as stated before, and translates into a high signal to noise ratio of the device, 7.2×10^{-2} at 30 mA.

In Figure 4.11, it is possible to find the response to the X-ray exposure of the diF TEG ADT device onto PEN. The analysis is very similar to the diF TES ADT on PEN. The sensitivity of the device is higher reaching 53.4 nC/Gy, which goes, once again, accordingly to what was expected given the germanium's higher Z number. The photocurrent has an even more linear increase with the dose rate than the diF TES ADT device with low error.

Once again, the bias stress is present in the highest dose (52.5 mGy/s), but it is still not significant enough to be a real problem for the measurement or the detector performance.

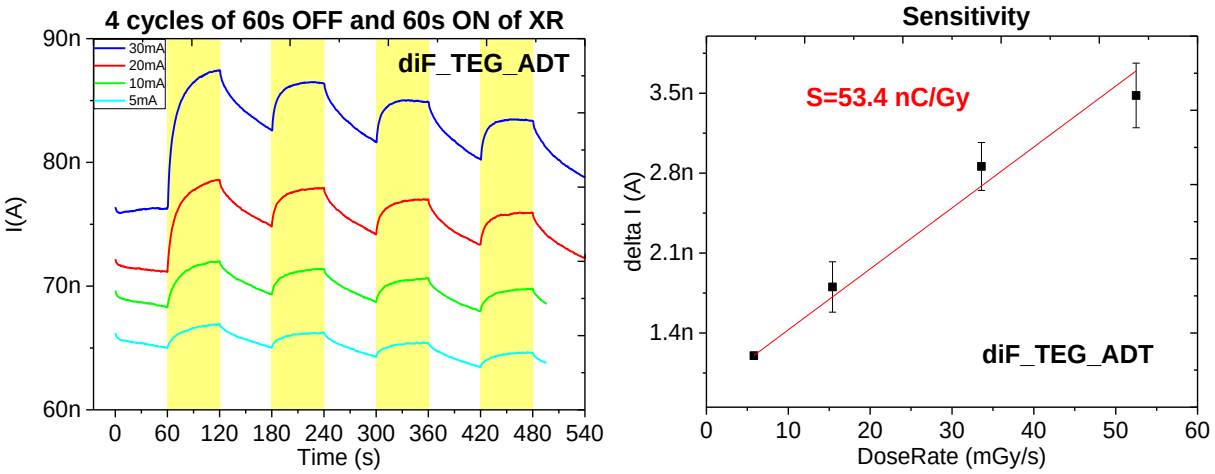

Figure 4.11: a) Dynamical behaviour of the current at different dose rates and b) Photocurrent vs Dose Rate of the best diF TEG ADT detector in PEN.

The response time is similar to the diF TES ADT device and so is the signal to noise ratio, being 4.3×10^{-2} at 30 mA.

In Table 4.2, the maximum current and sensitivity of all the detectors fabricated with the diF TES ADT and diF TEG ADT molecules on PEN are reported. The values in red are those that correspond to the presented graphs and, therefore to the best detectors.

With the diF TES molecule, the lowest maximum current corresponds to the highest sensitivity (S2). Nevertheless, with the other samples it seems that the highest the maximum current, the better the sensitivity. Therefore, this sample (S2) probably had a higher percentage of covered area with the molecule. It is possible to conclude that even if the sensitivity is not extremely high, the devices are reproducible and reliable because there is no discharge, there is no significant electrical stress, the photocurrent is constant with the increasing of the cycle of exposure and increases linearly with the dose rate.

The diF TEG ADT molecule in this substrate works quite well. As we can see in Table 4.2 there were two samples that reached similar sensitivities (S7 and S9) and had also really similar currents at 1 V. The other sample (S8) had a current at 1 V of half the value of the other two devices, and had a sensitivity of half the value of the others also. There must be then a linear relation here between the current achieved and the sensitivity reached.

Table 4.2: Sensitivity and maximum current of all the detectors based on diF TES ADT and diF TEG ADT on PEN.

Molecule	Sample	Imax (1V) (nA)	Sensitivity (St)(nC/Gy)
TES	**S2**	**8**	**13.3**
	S3	30	10.3
	S4	24	7.6
TEG	S7	997	50.0
	S8	418	20.9
	S9	**970**	**53.4**

4.2.3 Optical microscope

In Figure 4.12, the microscope pictures of the diF TES ADT and diF TEG ADT based detectors on PEN can be found. The thin films demonstrate, once again, good crystallization with aligned crystals.

With diF TES ADT the crystallization is not uniform. In the same sample it is possible to find areas with high crystallization, low crystallization and no crystallization at all. On the other hand, with diF TEG ADT it is possible to find big individualized crystals but not well aligned. This proves, once again, that the crystallization process is crucial in achieving a high performance device. Parameters like percentage of covered area of the device by the organic molecule, size and orientation of the crystals seem to have a big impact on the sensitivity of the device.

According to these results, these molecules have a better adhesion to the PEN substrate than to the PET substrate which leads to a higher and more linear sensitivity of the devices.

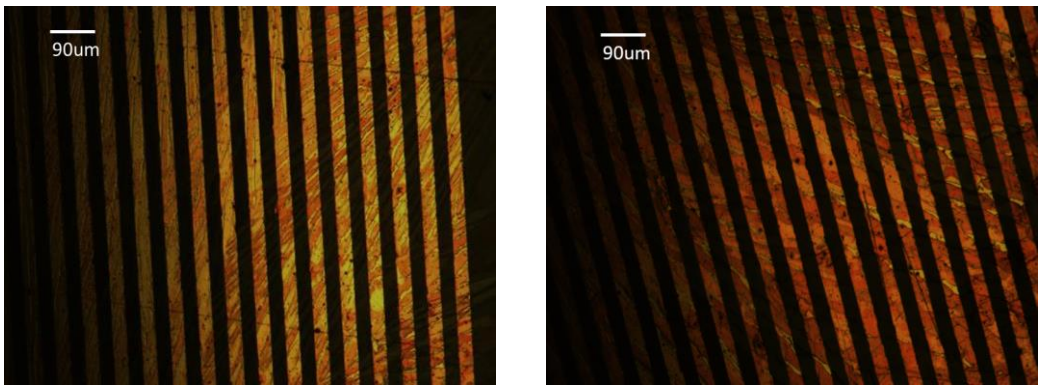

a b

Figure 4.12: Microscope pictures of a) diF TES ADT based detector and b) diF TEG ADT based detector onto PEN.

4.3 Glass substrate

Three devices were made onto the glass substrate, one with diF TES ADT and two with diF TEG ADT. Only one of these worked (diF TEG ADT).

The electrical characterization of the one working device is presented in Figure 4.13a. The maximum current at 1 V was 160 nA, which translates into a sheet resistivity of the 4.3×10^{10} Ω□.

In Figure 4.13b and c, the dynamical response to the radiation exposure of the diF TEG ADT detector on glass is reported. The sensitivity achieved is quite low, 2.6 nC/Gy. The photocurrent does not have a linear increase with the dose rate and the measurement seems quite noisy. The signal to noise ratio is, in this case, 3.0×10^{-2}. The device does not suffer from bias stress.

This is unexpected since, glass worked so well in the previous section with the TIPGe, and should therefore be the best substrate in terms of stability and reproducibility.

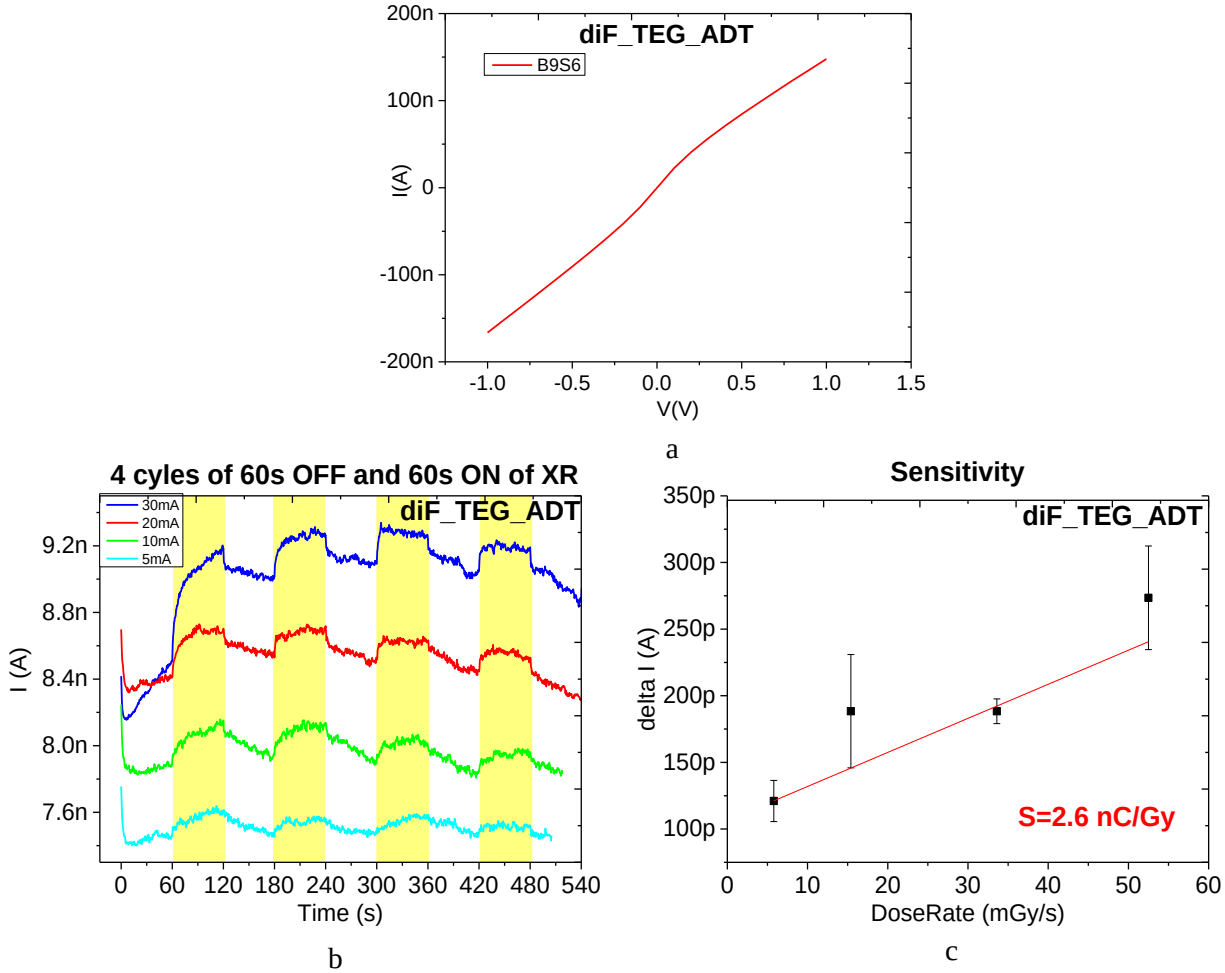

Figure 4.13: a) I-V characteristic, b) Dynamical behaviour of the diF TEG ADT detector on glass at different dose rates and c) Photocurrent vs Dose Rate of the same detector.

In Figure 4.14, it is possible to find the answer to the poor sensitivity of this device and probably to why the other two did not work. As we can see by the microscope picture there is simply no crystallization. There are only large gatherings of the molecule.

Figure 4.14: Microscope pictures the diF TEG ADT based detector on glass.

These results are not conclusive since there is such a low sample population. A deeper study on this type of detectors is necessary for further conclusions.

4.4 Summary

In Table 4.3, a summary of the most important parameters of the best diF TES ADT and diF TEG ADT based detectors on the three substrates tested is presented. The sensitivity per active area was calculated so the substrates could be compared having into consideration that they do not have the same dimensions.

Table 4.3: Summary of the most important parameters of the best detector based on diF TES ADT and diF TEG ADT on PET, PEN and glass.

Substrate	Molecule	Imax (1V) (nA)	Sheet Resistivity (Ω)	Total Sensitivity (St)(nC/Gy)	St/ActiveArea (nC/Gy.cm^2)	(S/N) at 30mA
PET	TES	1260	1.3×10^{9}	12.2	60.8	8.0×10^{-3}
	TEG	2870	5.8×10^{8}	3.3	16.5	1.3×10^{-3}
PEN	TES	8	9.1×10^{11}	13.3	75.9	7.2×10^{-2}
	TEG	970	7.1×10^{9}	53.4	305.1	4.3×10^{-2}
Glass	TES	-	-	-	-	-
	TEG	160	4.3×10^{10}	2.6	14.7	3.0×10^{-2}

The most important finding with this molecule was that it could have problems of adhesion to some surfaces and therefore the substrate should be chosen very carefully having into account the final application.

With the PET substrate, there is a strong discharge process with the first exposure of radiation. Not all the devices respond after that, and the ones who do present a big decrease in the current, even without X-Ray, due to the electrical stress, which results in a lower calculated sensitivity.

With the PEN substrate, there is a much better adhesion to the organic molecules proved by the microscope pictures that show really high quality crystals. This is translated in reliable and reproducible devices. The highest sensitivity achieved was with this substrate with the diF TEG ADT, 305.1 $nC/Gy.cm^2$.

The glass substrate did not work for the diF TES ADT molecule, and worked poorly for diF TEG ADT and it is necessary a deeper study on this type of detectors in order to understand if there is really a problem with this combination molecule/substrate.

5 Conclusions

In this project, four different molecules (TIPS, TIPGE, diF TES ADT and diF TEG ADT) were investigated as detectors of X radiation. The influence of different parameters in the sensitivity and, therefore, in the performance of the X-Ray detector were studied and can be found in Table 5.1.

Table 5.1: Summary of important parameters of the best detectors of TIPS, TIPGe, diF TES ADT and diF TEG ADT on PET, PEN and glass.

Substrate	Molecule	Imax (1V) (nA)	Sheet Resistivity (Ω)	Total Sensitivity (St)(nC/Gy)	St/ActiveArea (nC/Gy.cm^2)	(S/N) at 30mA
PET	TES	1260	1.3×10^{9}	12.2	60.8	8.0×10^{-3}
	TEG	2870	5.8×10^{8}	3.3	16.5	1.3×10^{-3}
PEN	TIPS	7	1.1×10^{12}	7.5	43.0	4.1×10^{-1}
	TIPGe	31	2.2×10^{11}	29.6	170.0	2.9×10^{-1}
	TES	8	9.1×10^{11}	13.3	75.9	7.2×10^{-2}
	TEG	**970**	$\mathbf{7.1\times10^{9}}$	**53.4**	**305.1**	$\mathbf{4.3\times10^{-2}}$
Glass	TIPS	160	4.3×10^{10}	7.9	46.0	2.5×10^{-1}
	TIPGe	195	3.5×10^{10}	80.7	461.0	3.1×10^{-1}
	TES	-	-	-	-	-
	TEG	160	4.3×10^{10}	2.6	14.7	3.0×10^{-2}

An important conclusion to take is that, in fact, as it was expected, the germanium instead of the silicon in the molecule makes a big difference in the results. Moreover, it was found that not only the Z number had an influence in the better performance of the TIPGe and diF TEG ADT, but also its high quality crystals. Only in one of the cases this was not observed and it was easily explained with another important parameter, the percentage of covered active area by the molecule. This proves that the crystallization process is a crucial one in achieving a high performance device as the dimension, quantity and orientation of the thin film crystals seem to have a major impact on the sensitivity of the detectors.

With the PET substrate, a discharge process was observed due to trap states that seem to induce a decrease in the current and therefore reduces both the dark current and the photocurrent. With the diF TES ADT and diF TEG ADT on PET, problems of crystallization inside the channel were spotted which could also explain the low sensitivities achieved.

With the PEN substrate, there is a better adhesion of the organic molecules proved by the microscope pictures that show high quality crystals. This is translated in reliable and reproducible devices with high signal to noise ratios. The sensitivities achieved with this substrate are not extremely high but are acceptable. For all of these advantages, the best device, out of all the ones tried, would be the diF TEG ADT on PEN.

Finally, the glass substrate with the TIPGe would be the best one because it combines a high sensitivity with a trustworthy device. This substrate did not work for the diF TES ADT molecule, and worked poorly for diF TEG ADT but only 3 samples were manufactured. It is necessary a deeper study on this type of detectors in order to understand if there is really a problem with this combination molecule/substrate or if it was just related to those particular samples.

5.1 Future Perspectives

The next step in this investigation would be to develop an approach to address, read, amplify and identify pixels based on these planar structures, using oxide electronics. The addressing and layout of this readout circuit was already studied for the *i-FLEXIS (Integrated Flexible Photonic Sensor System)* project, Figure 5.1. At this stage, clean room processes optimization is being performed at FCT-NOVA to improve the yield of fabricated chips and enable their proper operation.

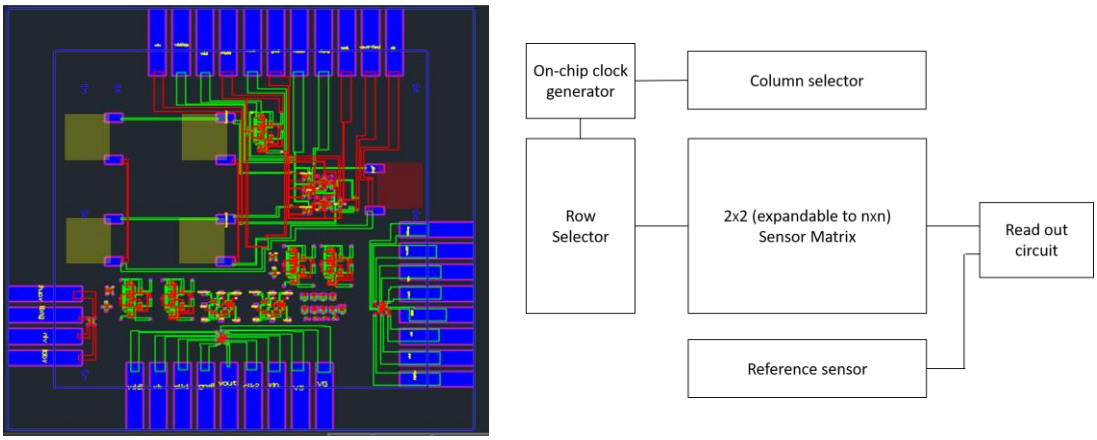

Figure 5.1: Addressing and layout of readout system.

Analyzing Figure 5.1, the yellow boxes would be glued with four X-Ray detectors which would be the ones that would be exposed to the radiation, while the red box would be glued with one detector that would always stay in the dark (reference sensor) based on the same organic molecule. In Table 5.1, it is possible to see (underlined in red) that the best detector would be the one based on diF TEG ADT on PEN, this being therefore the preferable combination for the implementation with the oxides chips.

The main goal would be to read the dose rate reaching each individualized detector. This would be done by creating an image in which each pixel corresponds to one detector and would portrait a color that would then be related to a dose rate.

Recently, there was an investigation that developed a circuit designed to match the electrical properties of organic thin film photoconductors acting as radiation sensors. In particular, it was targeting TIPS based detectors for their low dark current (10-100 nA), for a bias of less than 1 V and a photocurrent of 10 nA or less [44]. All these features are met with the best detector found in this project, so the TIPS could be replaced with the diF TEG ADT which would result in a more reliable device, not to mention an insurance on the similarity of the different detectors used onto the same substrate.

This combination between oxide electronics and the organic thin film photoconductors acting as radiation sensors needs to be tested and if successful improved and optimized. This would allow flexible, low-cost, large-area systems with low weight, suitable for wearable applications such as reliable X-ray systems for security purposes like radio therapy for cancer treatment or for laboratory workers, those who work in radiology and oncology departments, where real-time operation is often a demand for status alert. [44]

Bibliography

[1] L. Basiricò, A. Ciavatti, T. Cramer, P. Cosseddu, A. Bonfiglio, and B. Fraboni, "Direct X-ray photoconversion in flexible organic thin film devices operated below 1 V," *Nat. Commun.*, vol. 7, p. 13063, 2016.

[2] H. Minemawari *et al.*, "Inkjet printing of single-crystal films," *Nature*, vol. 475, no. 7356, pp. 364–367, 2011.

[3] G. Pipan *et al.*, "Direct Inkjet Printing of TIPS-Pentacene Single Crystals onto Interdigitated Electrodes by Chemical Confinement," *Adv. Mater. Interfaces*, vol. 5, no. 3, pp. 1–8, 2018.

[4] M. F. Toney and Z. Bao, "Tuning charge transport in solution-sheared organic semiconductors using lattice strain," *Nature*, vol. 480, pp. 504–509, 2011.

[5] Y. Diao *et al.*, "Solution coating of large-area organic semiconductor thin films with aligned single-crystalline domains," *Nat. Mater.*, vol. 12, no. 6, pp. 1–7, 2013.

[6] H. T. Yi, M. M. Payne, J. E. Anthony, and V. Podzorov, "Ultra-flexible solution-processed organic field-effect transistors," *Nat. Commun.*, vol. 3, no. May, pp. 1257–1259, 2012.

[7] S. Lai *et al.*, "A plastic electronic circuit based on low voltage, organic thin-film transistors for monitoring the X-Ray checking history of luggage in airports," *Org. Electron. physics, Mater. Appl.*, vol. 58, pp. 263–269, 2018.

[8] K. Yoshino, S. Hayashi, G. Ishii, and Y. Inuishi, "Electrical transport in electron beam irradiated polyacetylene," *Solid State Commun.*, vol. 46, no. 5, pp. 405–408, 1983.

[9] Nanomarkets, "Markets for Radiation Detection Equipment and Materials." 2013.

[10] P. Cosseddu, "Correlation between interface-dependent properties and electrical performances in OFETs," University of Cagliari, 2007.

[11] W. Brütting, "Introduction to the Physics of Organic Semiconductors," pp. 1–14, 2005.

[12] "What are the numbers of the pi and sigma bond in HCONHCH3?" [Online]. Available: https://www.quora.com/What-are-the-numbers-of-the-pi-and-sigma-bond-in-HCONHCH3. [Accessed: 12-Aug-2018].

[13] G. Mattana, "Realisation and Characterisation of Organic Electronic Devices for E – textiles applications," University of Cagliari, 2011.

[14] V. Coropceanu, A. Demetrio, S. Filho, Y. Olivier, R. Silbey, and J. Bre, "Charge Transport in Organic Semiconductors," pp. 926–952, 2007.

[15] B. Heinz and K. Anna, "Charge Transport in Organic Semiconductors," no. October 2011, 2012.

[16] A. S. Panchbhai, "Wilhelm Conrad Röntgen and the discovery of X-rays: Revisited after centennial," *J Indian Acad Oral Med Radiol*, vol. 27, no. 1, pp. 90–95, 2015.

[17] B. Fraboni, A. Fraleoni-Morgera, and N. Zaitseva, "Ionizing radiation detectors based on solution-grown organic single crystals," *Adv. Funct. Mater.*, vol. 26, no. 14, pp. 2276–2291, 2016.

[18] B. Fraboni, A. Ciavatti, L. Basiricò, and A. Fraleoni-Morgera, "Organic semiconducting single crystals as solid-state sensors for ionizing radiation," *Faraday Discuss.*, vol. 174, pp. 219–234, 2014.

[19] G. E. Knoll and J. Wiley, *Radiation Detection and Measurement Third Edition*. .

[20] K. K, “Ch 7 - Detecting nuclear radiations,” in *Introductory Nuclear Physics*, vol. 1, 1988, pp. 190–210.

[21] B. International, “The International System of Units (SI),” 2006.

[22] A. S. Saini and T. C. Zhu, “Dose rate and SDD dependence of commercially available diode detectors,” *Med. Phys.*, vol. 31, no. 4, pp. 914–924, 2004.

[23] A. Downloaded, N. York, Q. Chen, T. Hajagos, and Q. Pei, “Conjugated polymers for radiation detection,” pp. 298–318, 2011.

[24] J. P. Jones, “Improved Organic Scintillators in 2-Ethyl Naphthalene,” *Nature*, vol. 212, pp. 694–696, 1966.

[25] S. A. Payne *et al.*, “Nonproportionality of scintillator detectors: Theory and experiment. II,” *IEEE Trans. Nucl. Sci.*, vol. 58, no. 6 PART 2, pp. 3392–3402, 2011.

[26] P. E. Keivanidis *et al.*, “X-ray stability and response of polymeric photodiodes for imaging applications,” *Appl. Phys. Lett.*, vol. 92, no. 2, pp. 1–4, 2008.

[27] T. Agostinelli, M. Campoy-Quiles, J. C. Blakesley, R. Speller, D. D. C. Bradley, and J. Nelson, “A polymer/fullerene based photodetector with extremely low dark current for x-ray medical imaging applications,” *Appl. Phys. Lett.*, vol. 93, no. 20, pp. 2006–2009, 2008.

[28] B. Fraboni *et al.*, “Organic semiconducting single crystals as next generation of low-cost, room-temperature electrical X-ray detectors,” *Adv. Mater.*, vol. 24, no. 17, pp. 2289–2293, 2012.

[29] R. E. X. Detectors *et al.*, “Organic Semiconducting Single Crystals as Next Generation,” 2012.

[30] A. Intaniwet, J. L. Keddie, M. Shkunov, and P. J. Sellin, “High charge-carrier mobilities in blends of poly (triarylamine) and TIPS-pentacene leading to better performing X-ray sensors,” *Org. Electron.*, vol. 12, no. 11, pp. 1903–1908, 2011.

[31] C. A. Mills *et al.*, “Enhanced x-ray detection sensitivity in semiconducting polymer diodes containing metallic nanoparticles,” vol. 275102.

[32] H. Li, G. Giri, J. B.-H. Tok, and Z. Bao, “Toward high-mobility organic field-effect transistors: Control of molecular packing and large-area fabrication of single-crystal-based devices,” *MRS Bull.*, vol. 38, no. 01, pp. 34–42, 2013.

[33] S. K. Park, D. A. Mourey, S. Subramanian, J. E. Anthony, and T. N. Jackson, “High-mobility spin-cast organic thin film transistors,” *Appl. Phys. Lett.*, vol. 93, no. 4, 2008.

[34] K. Yang, “CONJUGATED POLYMERS AND SMALL MOLECULES WITH LATENT HYDROGEN-BONDING FOR ORGANIC ELECTRONIC APPLICATIONS,” University of Akron, 2017.

[35] A. E. Tonelli, “PET versus PEN : what difference can a ring make ? q,” vol. 43, pp. 637–642, 2002.

[36] O. D. Jurchescu *et al.*, “Organic single-crystal field-effect transistors of a soluble anthradithiophene,” *Chem. Mater.*, vol. 20, no. 21, pp. 6733–6737, 2008.

[37] K. I. Bolotin *et al.*, “Ultrahigh electron mobility in suspended graphene,” *Solid State Commun.*, vol. 146, no. 9–10, pp. 351–355, 2008.

[38] H. B. Akkerman, H. Li, and Z. Bao, “TIPS-pentacene crystalline thin film growth,” *Org. Electron. physics, Mater. Appl.*, vol. 13, no. 10, pp. 2056–2062, 2012.

[39] W. A. MacDonald *et al.*, “Latest Developments In Polyester Film For Flexible Electronics,” *SID Symp. Dig. Tech. Pap.*, vol. 36, no. 1, p. 514, 2005.

[40] M. Physics, “Role of Charge – carrier Trapping in Organic,” vol. 2, pp. 279–319, 2017.

[41] H. Search, C. Journals, A. Contact, M. Iopscience, and I. P. Address, “Barrier heights and surface states of metal-polymer,” vol. 2253.

[42] L. D. Faller, “Relaxation phenomenon.” [Online]. Available: https://www.britannica.com/science/relaxation-phenomenon. [Accessed: 27-Aug-2018].

[43] H. J. Butt, B. Cappella, and M. Kappl, “Force measurements with the atomic force microscope: Technique, interpretation and applications,” *Surf. Sci. Rep.*, vol. 59, no. 1–6, pp. 1–152, 2005.

[44] P. G. Bahubalindruni *et al.*, “High-Gain transimpedance amplifier for flexible radiation dosimetry using InGaZnO TFTs,” *IEEE J. Electron Devices Soc.*, vol. 6, no. March, pp. 760–765, 2018.